



# Evaluation of Potential Neuroprotective Effects of Vanillin Against MPP<sup>+</sup>/MPTP-Induced Dysregulation of Dopaminergic Regulatory Mechanisms in SH-SY5Y Cells and a Mouse Model of Parkinson's Disease

Linchi Rani<sup>1</sup> · Balaram Ghosh<sup>2</sup> · Mir Hilal Ahmad<sup>1</sup> · Amal Chandra Mondal<sup>1</sup>

Received: 23 June 2022 / Accepted: 18 April 2023 / Published online: 5 May 2023  
© The Author(s), under exclusive licence to Springer Science+Business Media, LLC, part of Springer Nature 2023

## Abstract

Parkinson's disease (PD) is a progressive neurodegenerative condition. The pathogenesis of PD is still unknown, and drugs available for PD treatment either have side effects or have suboptimal efficacy. Flavonoids are potent antioxidants having little toxicity with extended use, suggesting they might hold promising therapeutic potential against PD. Vanillin (Van) is a phenolic compound that has exhibited neuroprotective properties in various neurological disorders, including PD. However, the neuroprotective role of Van in PD and its underlying mechanisms are scarce and therefore need more exploration. Here, we evaluated the neuroprotective potential of Van and its associated mechanisms against MPP<sup>+</sup>/MPTP-induced neuronal loss in differentiated human neuroblastoma (SH-SY5Y) cells and the mouse model of PD. In the present study, Van treatment significantly enhanced the cell viability and alleviated oxidative stress, mitochondrial membrane potential, and apoptosis in MPP<sup>+</sup>-intoxicated SH-SY5Y cells. Moreover, Van significantly ameliorated the MPP<sup>+</sup>-induced dysregulations in protein expression of tyrosine hydroxylase (TH) and mRNA expressions of GSK-3 $\beta$ , PARP1, p53, Bcl-2, Bax, and Caspase-3 genes in SH-SY5Y cells. Similar to our in vitro results, Van significantly alleviated MPTP-induced neurobehavioral dysregulations, oxidative stress, aberrant TH protein expressions, and immunoreactivity in SNpc of mice brains. Treatment of Van also prevented MPTP-mediated loss of TH-positive intrinsic dopaminergic neurons to SNpc and TH-fibers projecting to the striatum of mice. Thus, Van exhibited promising neuroprotective properties in the current study against MPP<sup>+</sup>/MPTP-intoxicated SH-SY5Y cells and mice, indicating its potential therapeutic properties against PD pathology.

**Keywords** Vanillin · MPP<sup>+</sup>/MPTP · Apoptosis · Oxidative stress · Tyrosine hydroxylase · Parkinson's disease

## Abbreviations

AO	Acridine orange	DCF	2',7'-Dichlorofluorescein
AD	Alzheimer's disease	DAB	Diaminobenzidine
ANOVA	One-way analysis of variance	DAT	Dopamine transporters
BSA	Bovine serum albumin	DMEM	Dulbecco's modified Eagle's medium
BHT	Butylated hydroxytoluene	Ellman's reagent	5,5'-Dithiobis-(2-nitrobenzoic acid)
CAT	Catalase	FBS	Fetal bovine serum
DCFH-DA	2-7-Diacetyl dichlorofluorescein	GSH	Glutathione
DCFH	2', 7'-Dichloro-dihydrofluorescein	H&E	Hematoxylin-Eosin
		SH-SY5Y	Human neuroblastoma cells
		H <sub>2</sub> O <sub>2</sub>	Hydrogen peroxide
		LPO	Lipid peroxidation
		$\Delta\psi_m$	Mitochondrial membrane potential
		MPTP	1-Methyl-4-phenyl-1,2,3,6-tetrahydropyridine
		MPP <sup>+</sup>	1-Methyl-4-phenylpyridinium
		MTT	3-(4,5-Dimethylthiazol-2-yl)-2,5-diphenyltetrazolium bromide

✉ Amal Chandra Mondal  
acmondal@mail.jnu.ac.in

<sup>1</sup> Laboratory of Cellular and Molecular Neurobiology, School of Life Sciences, Jawaharlal Nehru University, New Delhi, India 110067

<sup>2</sup> Midnapore Medical College and Hospital, West Medinipur, Kolkata, West Bengal, India

NGS	Normal goat serum
NO	Nitric oxide
6-OHDA	6-Hydroxydopamine
OPA	Orthophosphoric acid
PFA	Paraformaldehyde
PD	Parkinson's disease
PBS	Phosphate buffer saline
PI	Propidium iodide
PARP	Poly (ADP-ribose) polymerase
PMS	Post mitochondrial supernatant
Pyrogallol	1,2,3-Trihydroxy benzene
RA	Retinoic acid
ROS	Reactive oxygen species
SNpc	Substantia nigra paras compacta
SOD	Superoxide dismutase
TBA	Thiobarbituric acid
TBARS	Thiobarbituric acid reactive substance
TH	Tyrosine hydroxylase
Van	Vanillin

## Introduction

Parkinson's disease (PD) was identified in 6.1 million people globally in 2016 and 2.4 times more than in 1990. Furthermore, it is predicted that by 2040, the number of cases will approach 12 million [1]. This steep rise is primarily due to higher life expectancy, as PD is rare in people under 50, predominantly affecting those over 60 and increasing rapidly beyond 75 [2]. Most PD symptoms are characterized by motor dysfunctions such as bradykinesia, postural instability, muscular rigidity, and resting tremor associated with the progressive degeneration of dopaminergic neurons in the substantia nigra pars compacta (SNpc) and subsequent dopamine depletion in the basal ganglia [3]. The precise mechanism that causes PD is unclear; however, oxidative stress, mitochondrial dysfunction, and apoptosis have been strongly linked to the disease pathophysiology [4]. Dysregulation of the tyrosine hydroxylase (TH) enzyme, which impairs dopamine production, has also been linked to PD-like symptoms [5]. TH, a rate-limiting enzyme of catecholamine synthesis, catalyzes the initial step of a biosynthetic pathway in the hydroxylation of tyrosine to L-DOPA. Phosphorylation and dephosphorylation of the TH enzyme reflect post-translational regulatory processes of the enzymatic activity regulating catecholamine levels in a dopaminergic system [6]. Therefore, TH activity is crucial for the development of catecholaminergic neurons. A dysfunctional catecholaminergic system, like the abnormal dopaminergic system, has been implicated in the pathogenesis of PD. PD-like symptoms have been observed due to dysregulation in TH activity and the resulting impairment of dopamine production [7]. Although the exact causes of PD remain unknown, numerous

environmental risk factors, especially neurotoxins, have been implicated in its etiology. Several neurotoxins, including 6-hydroxydopamine (6-OHDA), 1-methyl-4-phenyl-1,2,3,6-tetrahydropyridine (MPTP), rotenone, and paraquat have been developed to cause the degeneration of nigrostriatal dopaminergic neurons experimentally [8]. MPTP, in particular, has been extensively used in animal models of PD because it induces neuropathological changes similar to those that are observed in human PD [9]. It can cross the blood–brain barrier and cause dopaminergic neuronal damage in the SNpc and striatum by inducing a cascade of insults, including oxidative stress, mitochondrial aberrations, apoptosis, repression, and dysregulation of the dopamine synthesis enzyme TH, all of which act separately and in concert to cause damage in dopaminergic neurons [10]. MPTP is not itself toxic, but it is transformed into the active metabolite 1-methyl-4-phenylpyridinium (MPP<sup>+</sup>) by the monoamine peroxidase enzyme. MPP<sup>+</sup> later binds to dopamine transporters (DAT), inhibiting dopamine uptake and causing its depletion at cerebral levels. MPP<sup>+</sup> accumulates inside SNpc dopaminergic neurons after systemic administration. It enters the mitochondria and dysregulates oxidative phosphorylation by inhibiting complex I (NADPH-ubiquinone oxidoreductase I) in the electron transport chain. This results in the generation of free radicals, mitochondrial dysfunction, and impaired ATP production, leading to low cell energy and neuronal damage [11]. These superoxide radicals interact with nitric oxide (NO), generating peroxynitrite, a highly reactive tissue-damaging species that destroys proteins by oxidation and nitration, inducing dopaminergic neuronal death [12].

Dopamine replacement therapy with the dopamine precursor L-DOPA is the most commonly used treatment for PD [13]. Despite being regarded as the gold standard therapy for treating PD motor symptoms, L-DOPA is frequently associated with a variety of adverse side effects, the most common of which are motor fluctuations and dyskinesia [14]. Many additional therapeutic medications have their own limitations [15]. Since no effective drugs are currently available for restricting the loss of dopaminergic neurons in PD, novel therapeutic interventions with no side effects are required to overcome the disease severity. Recently, there has been a growing interest in phytochemicals exhibiting significant free radical scavenging activities and minimal toxicity even after prolonged usage, indicating that they might be potential innovative therapeutic strategies for PD [16].

Vanillin (4-Hydroxy-3-methoxy benzaldehyde) (Van), the active component of vanilla beans (*Vanilla planifolia*), is an anti-oxidative phytochemical that reduces reactive oxygen species (ROS) generation in a variety of neurological disorders, including PD [17]. Its beneficial effects are thought to be due to its antioxidant, anti-apoptotic, and anti-inflammatory properties, as well as its involvement with several signaling pathways that modulate neuronal differentiation and its

survival [18]. Van may also get across the blood–brain barrier [19]. Furthermore, it can block peroxynitrite-mediated processes, which are implicated in the etiology of various neurodegenerative disorders, including Alzheimer’s disease (AD) and PD [20]. The previous report suggests Van provided neuroprotection against 6-OHDA lesions by preserving striatal dopamine levels in a rat model of PD [17]. Van has also shown neuroprotection against rotenone-mediated neurotoxicity in SH-SY5Y cells [21]. The biological effects of Van are primarily attributed to the presence of phenolic, ether, and aldehyde moieties. Based on this, the current study sought to determine the neuroprotective effects of Van on mitochondrial aberrations, oxidative stress, and apoptosis in MPP<sup>+</sup>-exposed SH-SY5Y cells and a mouse model of PD. This study may provide a critical check into the factors through which PD progression expedites, which may provide a basis for future pre-clinical and clinical studies on PD.

## Materials and Methods

### Chemicals

MPP<sup>+</sup>, MPTP, Vanillin, 3-(4,5-dimethylthiazol-2-yl)-2,5-diphenyltetrazolium bromide (MTT), L-DOPA, 2–7-diacetyl dichlorofluorescein (DCFH-DA), Dulbecco’s modified Eagle’s medium (DMEM), EDTA, and Trypsin–EDTA were procured from Sigma Chemicals Co. (St. Louis, USA). Antibiotic/antimycotic were purchased from Hi-media. Fetal bovine serum (FBS) was obtained from Gibco. Acridine orange was obtained from SRL, and propidium was iodide obtained from life technologies. Mitochondrial Membrane Potential Assay Kit (JC-1) was obtained from Abbkine. Anti-TH was obtained from Novus biologicals, and Anti-NeuN antibody from Abcam. Goat anti-rabbit Alexa fluor-488 conjugated antibody (1:1000 dilution, ab150077, Abcam, USA).

### In Vitro Study

#### Cell Culture and Maintenance

SH-SY5Y cells were procured from the National Centre for Cell Science (NCCS), Pune, India, (passage 8). Cells were maintained in Dulbecco’s Modified Eagle Medium (DMEM) (Sigma Chemicals Co., USA), 10% fetal bovine serum (FBS) (Gibco Life Technologies, USA), and 1% antibiotic/antimycotic solution (HIMEDIA). Cultures were kept at 37 °C in a humidified incubator in an atmosphere of 5% CO<sub>2</sub> and 95% air. The cell culture media was replaced every 2 days, and the cells were sub-cultured when they reached 80–90% confluency. Following a 24-h incubation, cells were differentiated by adding 10 μM all-trans-retinoic acid (RA), dissolved in DMEM supplemented with 1% heat-inactivated FBS, and

incubated in the dark for 7 days at 37 °C with 5% CO<sub>2</sub> in an incubator. The RA-treated media were replaced every 2 days for 7 days, and morphological changes were visualized under a phase-contrast microscope (Eclipse Ti-E, Nikon) to monitor the differentiation and neurite length of undifferentiated and differentiated SH-SY5Y cells.

### Immunocytochemistry

Immunostaining of TH and NeuN was performed as per the study protocol [22] by plating differentiated SH-SY5Y cells on poly-D lysine-coated coverslips at a density of  $1 \times 10^4$  cells/coverslip and differentiated with 10 μM of RA for 7 days. Cells were then fixed in 4% paraformaldehyde (PFA) for 30 min at room temperature. Then, cultures were rinsed with PBS and incubated for 1 h in a blocking solution (3% BSA in 0.3% Triton X in PBS). After that, blocking was removed, and cells were incubated overnight at 4 °C with anti-TH antibody (Novus biological, Rabbit anti-TH, 1:1000 dilution in blocking solution) and anti-NeuN (ab177487 Rabbit anti-NeuN, 1:1000 dilution). Next day, cells were rinsed with PBS and incubated with secondary antibody (ab150077, Goat polyclonal Secondary Antibody to Rabbit IgG-H & L (1:1000, Alexa Fluor® 488 conjugated, Abcam, USA) for 2 h. After that, cells were counterstained with DAPI for 10 min and visualized under a fluorescent microscope (Eclipse Ti-E, Nikon).

### Cell Survival Assay

The MTT assay was used to evaluate the viability of SH-SY5Y cells. In a complete tissue culture medium, cells were seeded onto 96-well plates ( $1 \times 10^4$  cells/well) and cultured for 24 h. MPP<sup>+</sup> at concentrations 100 μM–1.5 mM and Van at concentrations 10–350 μM were given for 24 h to SH-SY5Y cells. Twenty-four hours after the treatments, the cells were incubated with a 20 μl MTT stock solution (5 mg/ml) for 4 h. MTT solution was extracted, and 100 μl DMSO was added to each well to dissolve the residual MTT formazan crystals. The absorbance was taken at 570 and 650 nm using a microplate reader. The results are expressed as a percentage of the control. Based on our MTT results and previous research findings [23], 1 mM of MPP<sup>+</sup> and 250 μM of Van were considered for in vitro experiments. The impact of Van on MPP<sup>+</sup>-induced cytotoxicity was determined following a similar procedure by incubating cells with MPP<sup>+</sup> (1 mM), Van (250 μM), and MPP<sup>+</sup> (1 mM) + Van (250 μM).

### Intracellular ROS Measurement

The amount of endogenous ROS production in control and treated cells were determined using the fluorescent dye DCFH-DA (Sigma Aldrich, USA). When it enters the cells,

DCFH-DA is deacetylated by cellular esterase to non-fluorescent 2', 7'-dichlorodihydrofluorescein (DCFH), which intracellular ROS rapidly oxidizes into the fluorescent 2',7'-dichlorofluorescein (DCF). The intensity of the DCF was used as a proxy for overall ROS production. SH-SY5Y cells were seeded ( $5 \times 10^5$  cells/well) in 6-well tissue culture plates and incubated for 24 h in a 5% CO<sub>2</sub> incubator maintained at 37 °C. Cells were exposed to MPP<sup>+</sup> (1 mM), Van (250 μM), and MPP<sup>+</sup> + Van concentrations at 37 °C for 24 h. The cells were treated with 10<sup>-3</sup> M DCFH-DA and incubated in the dark for 30 min after the treatment. After incubation, cells were rinsed with phosphate-buffered saline (PBS) to remove excess probe before being suspended in PBS and examined under a fluorescence microscope (Eclipse Tie-E, Nikon) at 20× magnification. The values are represented as the mean fluorescence intensity relative to the control wells.

According to the manufacturer's instructions, the mitochondrial superoxide analysis was performed using the MitoSOX™ Red mitochondrial superoxide indicator (Invitrogen). In brief, SH-SY5Y cells were seeded in a 12-well tissue culture plate and incubated for 24 h in a 5% CO<sub>2</sub> incubator maintained at 37 °C. Cells were treated with MPP<sup>+</sup> (1 mM), Van (250 μM), and MPP<sup>+</sup> + Van concentrations. After 24 h, cells were washed with HBSS twice, incubated with 5 μM MitoSOX-Red for 10 min at 37 °C in a 5% CO<sub>2</sub> atmosphere, followed by washing with HBSS twice to remove the excess probe, and finally examined under a fluorescence microscope (Eclipse Ti-E, Nikon).

#### Estimation of Mitochondrial Membrane Potential ( $\Delta\Psi_m$ )

The fluorescence intensity of cells stained with the JC-1 dye was used to evaluate  $\Delta\Psi_m$  as per the instructions in the kit. In brief, SH-SY5Y cells were seeded in 24-well plates ( $0.05 \times 10^6$ ) and incubated in a CO<sub>2</sub> incubator at 37 °C for 24 h before treatment. Cells were exposed to MPP<sup>+</sup> (1 mM), Van (250 μM), and MPP<sup>+</sup> + Van. Following treatment, JC-1 staining solution was added to each well and incubated in the dark for 15–30 min at 37 °C. Cells were rinsed twice with PBS after incubation and resuspended in a pre-warm DMEM medium. Cells were visualized under a fluorescent microscope (Eclipse Ti-E, Nikon) at 10× magnification. The ratio of aggregated red JC-1 dimers to green JC-1 monomers was used to calculate  $\Delta\Psi_m$ .

#### Acridine Orange/Propidium Iodide (AO/PI) Double Staining

SH-SY5Y cells were plated at a density of  $2 \times 10^5$  cells/well on a 6-well plate. Then, 24 h after seeding, the cells were differentiated with RA (10 μM) for 7 days before the treatment. The differentiated cells were treated with MPP<sup>+</sup> (1 mM), Van (250 μM), and MPP<sup>+</sup> + Van for 24 h. After trypsinizing the cells, 10 μL of the cell suspension was combined with 10 μL of AO (50 μg/mL) and PI (50 μg/mL) and placed

on a glass slide. Cells were visualized under a fluorescent microscope (Eclipse Ti-E, Nikon) at 20× magnification for morphological analysis.

#### Apoptosis Detection by Flow Cytometry

Apoptosis assay was performed using the Annexin V-FITC Apoptosis Detection Kit (Dead Cell Apoptosis Kits with Annexin V for Flow Cytometry, Invitrogen™) according to the manufacturer's protocol. Briefly, cells were plated in six-well plates and incubated for 24 h and then exposed to the desired concentrations of MPP<sup>+</sup>, Van, and MPP<sup>+</sup> + Van, for 24 h. Cells were then harvested and washed with PBS. After staining with a combination of Annexin V-FITC and PI, cells were immediately analyzed by flow cytometry (BDFACS Aria™ Fusion).

#### Analysis of mRNA Through qRT-PCR

The mRNA expressions were determined according to our previously adopted procedure [24]. Total mRNA was extracted from SH-SY5Y cells using the GeneJET RNA Purification kit (ThermoFisher Scientific). Optical density measurements determined the quantity and purity of RNA at A260/A280 ratio of 1.8 or above using a Nanodrop 2000 spectrophotometer (Thermo Fisher Scientific Inc., Wilmington, DE, USA). Following the manufacturer's instructions, the cDNA was synthesized from 1 μg of RNA using a Verso cDNA synthesis kit (ThermoFisher Scientific) and stored at –20 °C until assay. PowerUp™ SYBR™ Green Master Mix (Thermo Fisher Scientific) was used for RT-PCR quantification. The 20 μL reaction mixture contained a 20 ng cDNA template, 10 μL of SYBER GREEN master mix, 0.5 μL of forward primer, reverse primer, and PCR-grade water. GAPDH was used as a housekeeping reference gene. The primers for the qRT-PCR have the following sequences:

GSK-3β FP- GCTTCAACCCCAACAAATGC

RP- CCAAAACGTGACCAGTGTTC

PARP-1: FP—GGCGATCTTGACCGAGTAG

RP—CCTTTGGGGTTACCCACTCC

p53: FP -TGACACGCTTCCCTGGATTG

RP – GCTCGACGCTAGGATCTGAC

Bax: FP—GCCCTTTTGCTTCAGGGTTT

RP- CATCCTCTGCAGCTCCATGT

Bcl-2: FP—CTTTGAGTTCGGTGGGGTCA

RP – GGGCCGTACAGTTCCACAAA

Caspase-3: FP—TGGAACCAAAGATCATACATGGAA



RP—TTCCCTGAGGTTTGCTGCAT

GAPDH: FP—AATGGGCAGCCGTTAGGAAA

RP – GCGCCCAATACGACCAAATC

The gene expression was determined by a 7500 Fast Real-time system (Software v2.0.5, Applied Biosystems) with 40 cycles in a fixed sequence of 95 °C for 30 s, 62 °C for 15 s, and 72 °C for 15 s. GAPDH was used as a reference control gene.

### Western Blot

Protein expression was determined as per our previous procedure [25]. Fifty micrograms of proteins were fractionated by SDS-PAGE and transferred onto the PVDF membrane. The blots were blocked and incubated with the primary antibody (anti-TH, 1:1000 dilutions, Novus Biologicals) at 4 °C overnight. Following this, membranes were incubated with Anti-rabbit HRP-conjugated secondary antibody (CST) diluted (1:1000) for 2 h at room temperature. The ECL method was employed to visualize the bands and X-ray film to detect protein signals. Densitometry was used to measure the expression of the target protein using ImageJ software, which was normalized using  $\beta$ -actin as an internal reference. The data are presented as a ratio of target protein expression in MPP<sup>+</sup>, Van, and MPP<sup>+</sup> + Van-treated groups to the control group.

### In Vivo Study

#### Animals and Diet

Male C57BL/6 mice (25–30 g; 10–12 weeks old) were housed in standard laboratory conditions, including an ambient temperature of  $21 \pm 2$  °C with 12-h light/dark cycle, 55% humidity, and free access to a standard rodent pellet diet and filtered water ad libitum. All animal-based research work was approved by the Central Laboratory Animal Resource (CLAR), JNU, New Delhi, India. Animals were acclimatized for 1 week before initiating the experimental protocol. Before the experiment, mice were trained on all behavioral equipment for ceiling performance. The timeline of the treatments and experiments is depicted in Fig. 8A.

#### Experimental Protocol

Adult male C57BL/6 mice were randomly divided into five experimental groups, each with 12 animals. Group 1 (control): Received normal saline (i.p.) used as a vehicle.

Group 2 (MPTP): MPTP was administered by i.p. injection once daily for five consecutive days [26]. Group 3 (Van): Received Van (60 mg/kg body weight, p.o.) dissolved in normal saline daily for 21 days. Group 4 (MPTP + Van): Received an i.p. injection of MPTP once a day for five consecutive days, followed by Van (60 mg/kg body weight, p.o.) daily for 21 days. Group 5 (MPTP + L-DOPA): Received i.p. injection of MPTP once a day for five consecutive days, followed by L-DOPA (5 mg/kg body weight, p.o.) each for 21 days.

### Assessment of Motor Behavior

Motor functions were assessed at the end of the dosing regime.

**Pole Test** The pole test identifies the severity of bradykinesia in PD [27]. Mice were placed head up on the top of a vertically positioned wooden pole to prevent them from slipping (diameter 8 mm and height 50 cm). The time taken to climb down with all 4 ft on the floor was calculated.

**Narrow Beam Test** Animals were permitted to walk on a narrow wooden beam (width 1 cm, length 100 cm) placed 100 cm above ground [28]. The time it took to traverse the beam from one end to the other and foot slip errors were recorded.

### Tissue Processing

After the functional assessment, experimental mice were anesthetized by i.p. thiopentone sodium (150 mg/kg body weight) and sacrificed by decapitation. The striatum and SNpc tissues were carefully dissected from mouse brains using the bregma as a reference landmark [29]. The isolated tissues were flash-frozen in liquid nitrogen and kept at  $-80$  °C until they were analyzed.

#### Measurement of Striatal MPP<sup>+</sup> Levels by HPLC

Striatal MPP<sup>+</sup> levels were measured by HPLC equipped with UV detectors, according to a previous study [26]. In brief, mice were injected with MPTP intraperitoneally (20 mg/kg) and orally administered with Van (60 mg/kg). After 90 min, the mice were sacrificed, and the striata were quickly dissected on ice and kept at  $-80$  °C until further processing. Tissue samples were then homogenized in 9 volumes of 5% TCA containing 10  $\mu$ g/ml internal standard (4-phenyl pyridine) and centrifuged at 15,000 g for 20 min at 4 °C. After centrifugation, 50  $\mu$ l of supernatant was injected into the C18 reverse column (5  $\mu$ m, 250  $\times$  4.6 mm) attached to the HPLC system (Agilent Technologies, 1220 Infinity LC) at a flow rate of 1.0 ml/min. The mobile phase consisted of 89% 50 mM potassium phosphate adjusted to pH 3.2 with

ultrapure 18 M phosphoric acid and 11% acetonitrile. MPP<sup>+</sup> was identified by comparison of retention time with known standards, and concentrations were calculated by generating standard curves.

## Biochemical Estimations

**Preparation of Post-Mitochondrial Supernatant (PMS)** All biochemical experiments were performed on six experimental mice in each group. To make a 10% tissue homogenate, tissue samples were homogenized in ice-cold 0.1 M PBS at pH 7.4. The procedure was carried out with a homogenizer at a medium speed for 8–10 strokes while the samples were kept on ice. Then, homogenates were centrifugated at 4 °C at 15,000 rpm for 20 min to obtain 10% PMS, which was then kept at –20 °C for further investigations.

**Estimation of Protein** The protein content of brain tissues was calculated using the Bradford et al. method. Bovine serum albumin (BSA) served as a standard reference [30].

**Analysis of the Enzymatic Activity of Superoxide Dismutase (SOD)** SOD activity was determined based on our previous method [31]. In brief, a pre-mixture was created by mixing 15 µl of 10% PMS with 3 µl of 12.5% Triton-X-100. The pre-mixture was incubated for 30 min at 4 °C. Following incubation, 15 µl of the pre-mixture was dissolved in 750 µl of 0.1 M phosphate buffer, 593.5 µl of double-distilled water, 49.5 µl of 3 mM EDTA (pH 8), and 90 µl of pyrogallol (1,2,3-trihydroxy benzene). The pyrogallol reaction mixture solution consisted of 10.2 mg of pyrogallol dissolved in 10 ml of double-distilled water and 8.6 µl of HCl. The resultant solution was gently mixed, and absorbance was measured kinetically using a spectrophotometer at 420 nm (Agilent Technologies' Cary 60 UV–Vis) at 1-min intervals for 3 min. SOD activity in each sample was measured in millimoles of inhibition of pyrogallol autoxidation per minute per milligram protein.

**Estimation of Catalase (CAT) Enzymatic Activity** CAT activity was measured by the method described by Fatima et al. [25]. Five hundred microliters of 0.05 M hydrogen peroxide (H<sub>2</sub>O<sub>2</sub>) was dissolved in a mixture comprising 25 µl of 10% PMS and 975 µl of 0.1 M phosphate buffer (pH 7.4) to prepare the reaction mixture. The resultant reaction mixture was gently agitated, and absorbance at 240 nm was kinetically measured every 1 min for 3 min. CAT activity was calculated as millimoles of H<sub>2</sub>O<sub>2</sub> used per minute per milligram of protein in each sample.

**Determination of Lipid Peroxidation (LPO) Level** LPO was estimated by using our previously adopted method [24]. Briefly, 88 µl of 10% PMS was mixed with 10 µl of 10 mM butylated

hydroxytoluene (BHT) and 350 µl of 0.67% thiobarbituric acid (TBA). After vortexing, 1 ml of 1% orthophosphoric acid (OPA) was added. The resultant mixture was incubated at 95 °C for 45 min in boiling water. The absorbance of each aliquot was measured on a spectrophotometer at 535 nm. The LPO levels were calculated as nanomoles of thiobarbituric acid reactive substance (TBARS) produced per hour per gram of tissue.

**Measurement of Reduced Glutathione (GSH) Level** GSH levels determined by our previously adopted method [25] were used to assess tissue GSH levels; this approach uses Ellman's reagent [5,5'-dithiobis-(2-nitrobenzoic acid)] to colorimetrically estimate GSH levels as total "acid soluble sulfhydryl" concentrations. Briefly, 10% PMS was precipitated with 4% sulphosalicylic acid in a ratio of 1:1. The samples were kept at 4 °C for 1 h and subjected to centrifugation at 5000 rpm for 15 min at 4 °C. Two hundred microliters of the resulting supernatant was mixed with 1.1 ml of 0.1 M phosphate buffer (pH 7.4). Finally, 200 µl Ellman's reagent (10 mM) was added, and the reaction mixture was gently stirred. The optical density was measured immediately at 412 nm, and results were calculated as micromoles of GSH per gram of tissue in each sample.

## Immunohistochemistry

Immunohistochemistry was performed based on our previously adopted method [32]. Animals were anesthetized with thiopentone sodium (150 mg/kg body weight, i.p.). After that, the mice were transcardially perfused with normal saline, followed by a fixative containing 4% PFA dissolved in PBS (0.1 M, pH 7.4). Tissues were fixed, cut into 20-µm thick slices with a cryotome, mounted on 1% gelatin-coated glass slides, and immunostained. Sections were blocked in a humid chamber for 1 h with 5% BSA and then incubated with anti-TH antibody (Novus biological, Rabbit anti-TH, 1:1000 dilutions) overnight at 4 °C. The next day, tissue sections were washed with PBS and incubated with secondary antibody (ab150077, Goat polyclonal Secondary Antibody to Rabbit IgG-H & L (1:1000, Alexa Fluor® 488 conjugated, Abcam, USA) at room temperature for 2 h and after that, counterstained with DAPI for 30 min. Tissue sections were then mounted and visualized under a fluorescent microscope (Eclipse Ti-E, Nikon) at 10× magnification. In each experimental group, four animals were used.

The sections were thawed in a hot air oven at 60 °C for 20 min before staining with 3,3-diaminobenzidine-4 HCL (DAB). They were then incubated at room temperature for 1 h. After incubation, tissue sections were rinsed with PBS and blocked with endogenous peroxidase (3% H<sub>2</sub>O<sub>2</sub> in 100% methanol) for 5–7 min. Tissues were rinsed again with PBS and blocked with 10% normal goat serum (NGS). Sections were incubated with the primary antibody (Novus biological, Rabbit

anti-TH, 1:1000 dilution) in 5% NGS blocking buffer overnight at 4 °C. The following day, sections were again rinsed and incubated with secondary antibody (Vector Laboratories anti-rabbit biotinylated secondary antibody cat#PK-4001 dilution 1:200) in 1% NGS blocking buffer overnight at 4 °C. After washing, sections were incubated in avidin-biotinylated horseradish peroxidase (ABC Kit, Vector Laboratories) in PBS for 30 min, rinsed, and developed with DAB (DAB peroxidase substrate kit, SK-4100, Vector Laboratories) in 0.05 M tris buffer (pH7.6). Slides were allowed to dry for 1 h at room temperature, dehydrated, mounted with DPX mounting medium, and visualized under a microscope (Nikon 80i).

### Histopathology in Mice Brain

**Nissl Staining** For Nissl staining, sections were dried overnight at room temperature and stained for 10–15 min with 0.1% cresyl violet solution. After staining, the slides were rinsed with distilled water and dehydrated with 70%, 90%, and 100% ethanol. Finally, the sections were cleared with xylene and mounted with a DPX mounting medium. A Nikon 80i microscope was used to examine the sample images.

**Hematoxylin and Eosin Staining** Histopathology was done using our previously described method [33]. The mice were anesthetized. Tissues were cut into thick Sects. (10 µm) using a cryotome after fixation. Hematoxylin–Eosin (H&E) stain was used to stain striatal slices of the brain. For neuro-anatomical details, the prepared slides were examined using a light microscope (Nikon 80i). For each mouse, eight sections of the striatum were examined ( $n = 4$ ).

### Cell Counting for Estimating TH Immunoreactive and Nissl Positive Neurons

Unbiased stereological cell counting was performed using the stereological method of optical fractionator [34]. Briefly, the number of TH immunoreactive and Nissl positive neurons from six serial sections of the SNpc was counted using a random offset grid (130 µm × 130 µm) and an unbiased counting frame (60 µm × 60 µm) using stereological morphometric grids developed by Aleksandr Mironov [35]. Thickness sampling fraction was 0.8 with 2-µm upper and 2-µm lower guard zones. Prior to stereological quantification, the investigator was blind to the distinction between the slides from different groups to ensure unbiased estimates. The number of neurons in the SNpc was estimated by multiplying the number of neurons counted within the sample regions by the reciprocals of the area sampling fraction and the fraction of the section sampled. The corresponding mean coefficient of error was equal to or less than 0.10 in all groups. Also, the density of the TH

immunoreactive-fibers was estimated by measuring the optical density using FIJI [36].

### Statistical Analysis

An observer blind to the research design and treatment condition throughout the experiment performed all behavioral scoring and examinations of the histopathological characteristics. GraphPad Prism software version 7 was used for the statistical analysis (GraphPad Software, USA). All data are presented as the mean ± SEM. To assess the significant differences between the control, MPTP, Van, MPTP + Van, and MPTP + L-DOPA groups, a one-way analysis of variance (ANOVA) was used, followed by a Tukey test that assumes the data has a normal distribution. To indicate significant differences when compared to the control, \* $p < 0.05$ , \*\* $p < 0.01$ , and \*\*\* $p < 0.001$  were used and # $p < 0.05$ , ## $p < 0.01$ , and ### $p < 0.001$  when compared to the MPP<sup>+</sup>/MPTP groups.

## Results

### Validation of Differentiation in SH-SY5Y Cells Using Neuronal Maturation Markers

The assessment of two neuron-specific markers validated the effective cellular differentiation: (a) NeuN, a nuclear marker for post-mitotic mature neurons and (b) TH, a rate-limiting enzyme for the dopaminergic neuronal marker in the differentiated cells. NeuN and TH expression (Fig. 1A and B) were elevated in RA-treated SH-SY5Y cells. The protein expression of TH determined the differentiation of SH-SY5Y cells into dopaminergic neurons. As clear from Fig. 1C, cells that were treated with RA expressed TH protein in contrast to the untreated and undifferentiated cells, suggesting the effective differentiation of SH-SY5Y cells into the dopaminergic neuron-like phenotype. As a result, we proceeded to use differentiated wild-type SH-SY5Y cells as a PD model.

### Van Inhibits MPP<sup>+</sup>-Induced Cytotoxicity in SH-SY5Y Cells

The MTT assay determined the cytotoxic effect of MPP<sup>+</sup> on the viability of SH-SY5Y cells by administrating increasing doses of MPP<sup>+</sup> (100 µM–1.5 mM) to differentiated SH-SY5Y cells. MPP<sup>+</sup> significantly reduces the viability of SH-SY5Y cells in a dose-dependent manner (Fig. 2A,  $F = 25.94$ ,  $p < 0.001$ ). MPP<sup>+</sup> administration at 1 mM dose for 24 h resulted in 50% cell viability of SH-SY5Y cells, which was considered for further experiments.

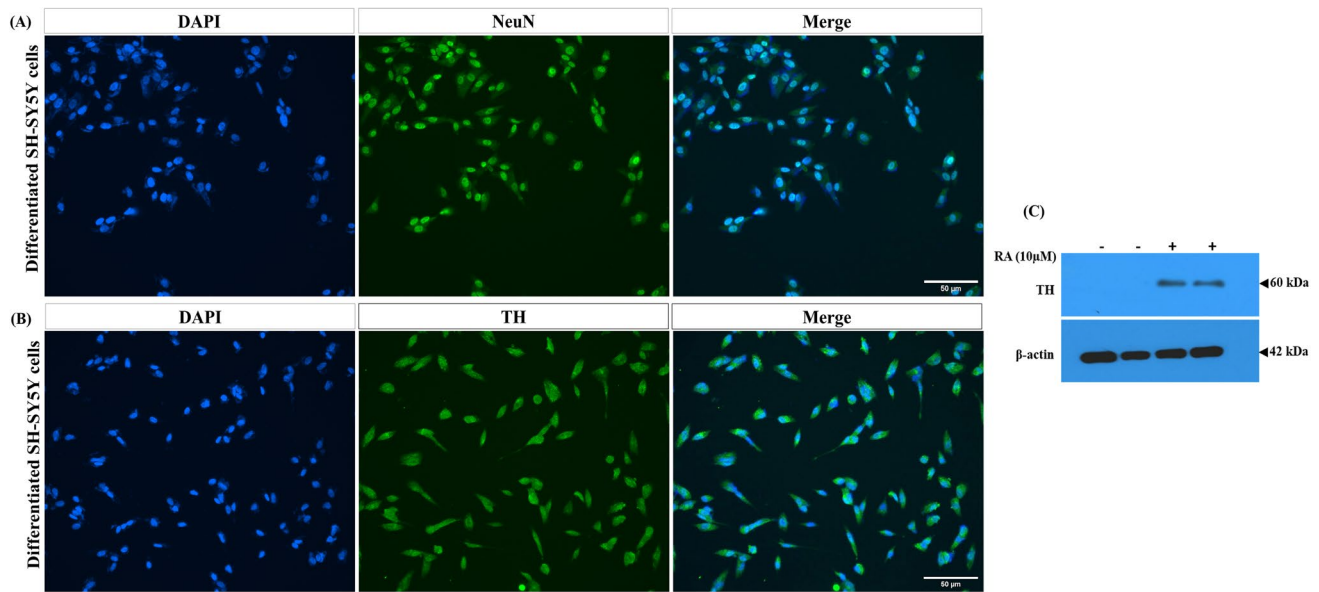


**Fig. 1** Expression of NeuN and TH in SH-SY5Y cells after differentiation with RA treatment. (A), (B) Representative immunofluorescence images for mature neuron-specific marker NeuN and dopaminergic neuronal marker TH in the cells treated with RA (10  $\mu$ M) for

7 days. Images were obtained using a fluorescent microscope (Eclipse Ti-E, Nikon) Scale bar, 50  $\mu$ m. (C) Effect of RA (10  $\mu$ M) treatment on protein expression of TH in differentiated SH-SY5Y cells

MTT assay was determined to investigate the dose-dependent (10–350  $\mu$ M) effect of Van in SH-SY5Y cells. Our findings reveal that Van was not toxic to SH-SY5Y cells in a concentration-dependent manner (Fig. 2B,  $F = 1.631$ ). However, the non-toxic effect of Van was slightly reduced at doses of 250  $\mu$ M or higher in SH-SY5Y cells.

We also performed MTT assay to determine the cytoprotective effect of Van on MPP<sup>+</sup>-induced neurotoxicity in SH-SY5Y cells. Cell viability assays revealed that MPP<sup>+</sup> treatment caused significant ( $p < 0.001$ ) cytotoxicity in SH-SY5Y cells compared to control cells. Compared to MPP<sup>+</sup>-treated SH-SY5Y cells, Van-treated cells showed a significant ( $p < 0.01$  and  $p < 0.001$ ) reduction in cellular toxicity. The cytoprotective effect of Van on SH-SY5Y cells diminished at concentrations greater than 250  $\mu$ M (Fig. 2C,  $F = 44.70$ ,  $p < 0.001$ ). There was a 1.59-fold increase in cell viability in Van-treated cells compared to the MPP<sup>+</sup>-administrated cells. Our MTT results showed that Van treatment significantly ( $p < 0.001$ ) enhanced cell survival in MPP<sup>+</sup>-administered cells, indicating a potential cytoprotective effect against MPP<sup>+</sup>-mediated intracellular cytotoxicity.

### Van Rescues MPP<sup>+</sup>-Mediated Intracellular ROS Generation in SH-SY5Y Cells

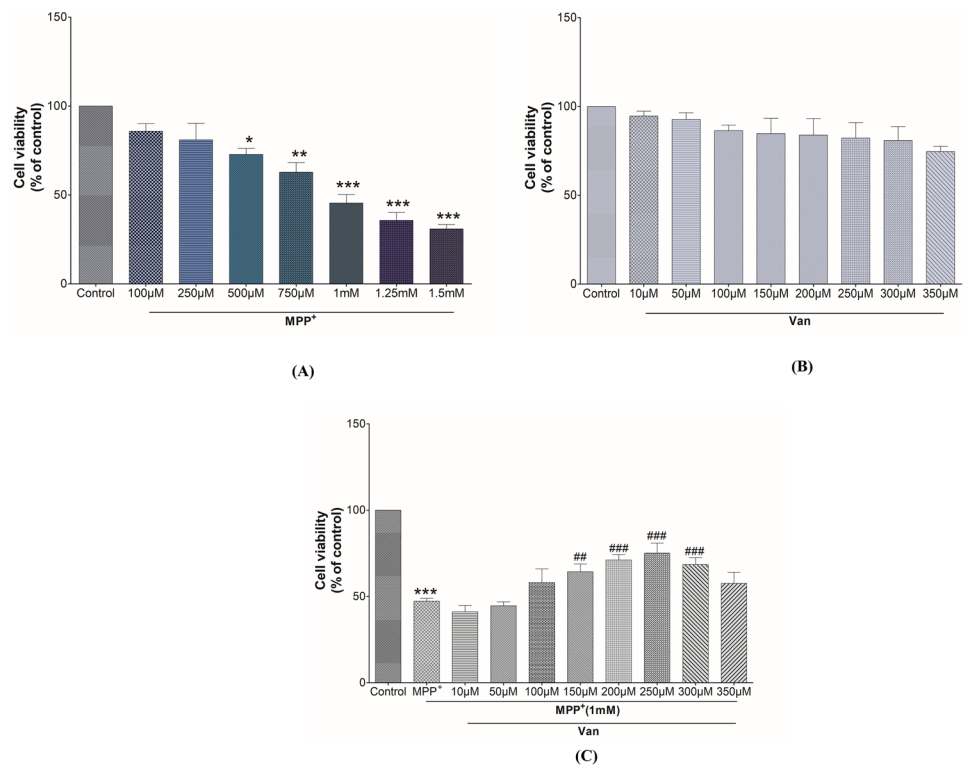
Since enhanced ROS generation is implicated in numerous neurodegenerative diseases, including PD, we evaluated the intracellular ROS level using the fluorescent probe DCFHDA. ROS generation in SH-SY5Y cells was

evaluated to see if Van suppresses ROS formation, followed by MPP<sup>+</sup> treatment. Following MPP<sup>+</sup> exposure, a significant increase in intracellular ROS levels was observed in SH-SY5Y cells when compared to the control cells, and the Van treatment significantly alleviated the MPP<sup>+</sup>-induced intracellular ROS formation. Our results show that DCF fluorescence was significantly ( $p < 0.001$ ) higher in MPP<sup>+</sup>-treated cells than in the control cells, indicating increased endogenous ROS generation. On the other hand, cells treated with Van showed a significant ( $p < 0.01$ ) reduction in the DCF fluorescence intensity, indicating decreased ROS production. Van treatment significantly reduced ROS production by 1.39-fold in comparison to the MPP<sup>+</sup>-treated cells (Fig. 3B,  $F = 34.61$ ,  $p < 0.01$ ). These findings confirm that Van provides cytoprotection by scavenging ROS caused by MPP<sup>+</sup>. The representative fluorescence images of DCFH-DA in the control, MPP<sup>+</sup>, Van, and MPP<sup>+</sup> + Van-treated groups are given in Fig. 3A.

These findings were further validated by MitoSOX red staining. MitoSOX primarily targets mitochondria and generates red fluorescence after being oxidized by superoxide. Consistent with prior DCFH-DA findings, there is a significant elevation in MitoSOX red fluorescence in MPP<sup>+</sup>-treated SH-SY5Y cells compared to the controls. The intensity of MitoSOX red fluorescence was significantly reduced in cells treated with Van. Our data indicate that MPP<sup>+</sup>-treated SH-SY5Y cells showed significantly ( $p < 0.01$ ) higher MitoSOX red fluorescence intensity than the control cells, suggesting an increase in superoxide



**Fig. 2** Effect of Van treatment on MPP<sup>+</sup>-induced cytotoxicity in SH-SY5Y cells and morphological appearance of differentiated SH-SY5Y cells with increasing concentrations of MPP<sup>+</sup> and Van. (A) Dose-response effect of MPP<sup>+</sup> treatment on SH-SY5Y cell viability as measured by MTT assay and expressed as a percentage of control. (B) Dose-dependent effect of Van treatment on SH-SY5Y cell viability. (C) Effect of MPP<sup>+</sup> administration and Van treatment on the viability of SH-SY5Y cells. Values are given as mean  $\pm$  SEM, \* $p$  < 0.05, \*\* $p$  < 0.01, and \*\*\* $p$  < 0.001 vs. control and ## $p$  < 0.01 and ### $p$  < 0.001 vs. MPP<sup>+</sup>



in mitochondria. When cells were treated with Van, the intensity of MitoSOX fluorescence alleviated significantly ( $p$  < 0.05), suggesting decreased superoxide production in mitochondria. Compared to the MPP<sup>+</sup>-administrated cells, Van treatment resulted in a 1.29-fold reduction in ROS production (Fig. 3D,  $F = 14.12$ ,  $p$  < 0.05). According to these findings, Van decreased MPP<sup>+</sup>-induced ROS production in mitochondria and exerted a free radical scavenging or antioxidant activity in MPP<sup>+</sup>-intoxicated SH-SY5Y cells. The representative MitoSOX fluorescence images from the control, MPP<sup>+</sup>, Van, and MPP<sup>+</sup> + Van-treated groups are shown in Fig. 3C.

### Van Ameliorates MPP<sup>+</sup>-Mediated Disruption of Mitochondrial Membrane Potential ( $\Delta\psi_m$ )

Dysregulation in  $\Delta\psi_m$  is one of the significant events during mitochondrial dysfunction. Therefore, we measured the neuroprotective effect of Van treatment against MPP<sup>+</sup>-induced  $\Delta\psi_m$  dysregulations in SH-SY5Y cells. Present results show that MPP<sup>+</sup>-treated cells exhibit lower red JC-1 dimers and higher green JC-1 monomers in mitochondria compared to the control, which confirms that MPP<sup>+</sup> treatment results in depolarization of  $\Delta\psi_m$ . In contrast, Van-treated SH-SY5Y cells exhibited increased production of red JC-1 dimers, demonstrating the restoration of  $\Delta\psi_m$ . MPP<sup>+</sup> treatment in SH-SY5Y cells caused a significant ( $p$  < 0.01) increase in  $\Delta\psi_m$  compared to the controls, whereas Van treatment resulted in

a 2.74-fold decrease in  $\Delta\psi_m$  compared to MPP<sup>+</sup>-treated cells (Fig. 4B,  $F = 10.47$ ,  $p$  < 0.05). The findings show that Van treatment significantly modulates the MPP<sup>+</sup>-induced disruption in  $\Delta\psi_m$ , implying that Van can restore MPP<sup>+</sup>-induced mitochondrial dysfunction by reducing  $\Delta\psi_m$ . Figure 4A shows JC-1Red/Green fluorescence representative images of the control, MPP<sup>+</sup>, Van, and MPP<sup>+</sup> + Van-treated groups.

### Van Protects Against MPP<sup>+</sup>-Induced Apoptosis in SH-SY5Y Cells

Double staining of AO/PI in SH-SY5Y cells treated with MPP<sup>+</sup> and Van was used to measure the number of apoptotic cells. The green-stained nucleus of the cells indicates cell viability, but those stained with red signify apoptosis. The results show the formation of the orange-red luminescent apoptotic body in MPP<sup>+</sup>-administered cells, representing apoptosis when compared to the control, which shows a green-stained nucleus, normal morphology, and viability. When these cells were treated with Van, most cells exhibited a green fluorescence and showed a normal appearance of intact cells. Our results show that Van treatment alleviates apoptosis in SH-SY5Y cells induced by MPP<sup>+</sup> administration. The representative images of AO/PI fluorescence in control, MPP<sup>+</sup>, Van, and MPP<sup>+</sup> + Van-treated groups are shown in Fig. 5A.

Annexin/PI dual staining also confirmed these similar findings. Our data shows that the percentage of apoptotic



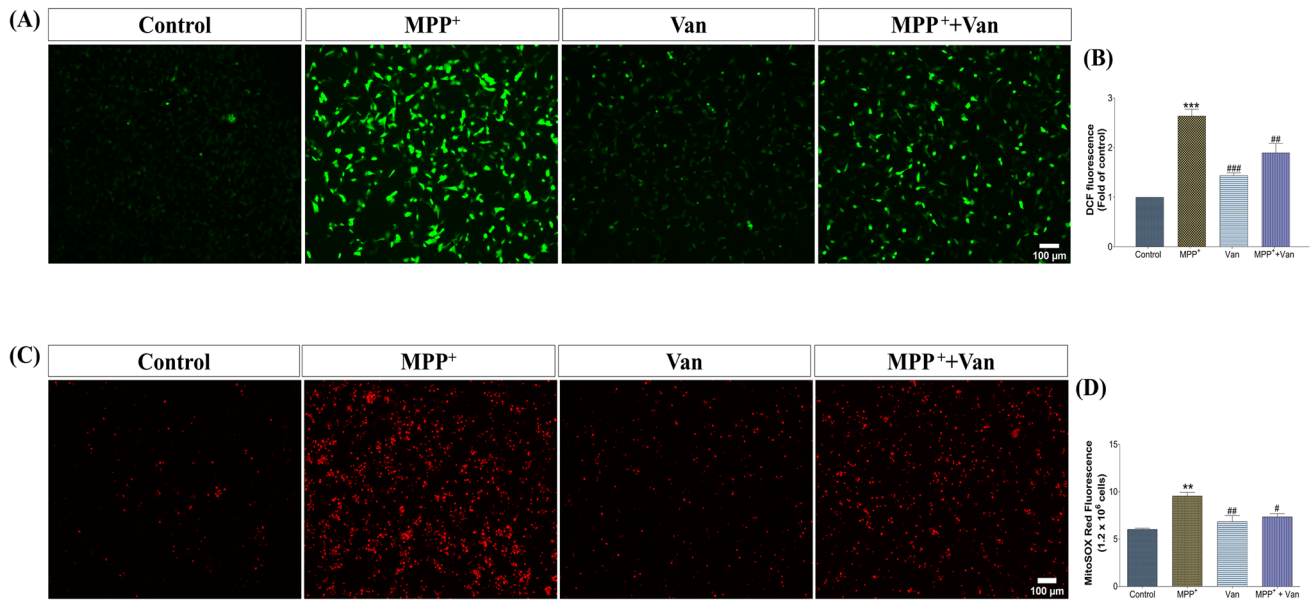


**Fig. 3** Effect of Van on oxidative stress in MPP<sup>+</sup>-induced SH-SY5Y cells and determining mitochondrial ROS level using MitoSOX Red. **(A)** Representative DCF fluorescence images of control, MPP<sup>+</sup>, Van, and MPP<sup>+</sup>+Van-treated group (scale bar: 100  $\mu$ m) **(B)** Bar graphs depicting relative DCF fluorescence intensity (fold of control) in control, MPP<sup>+</sup>, Van, and MPP<sup>+</sup>+Van-treated groups. **(C)** Repre-

sentative fluorescence images of MitoSOX red in control, MPP<sup>+</sup>, Van, and MPP<sup>+</sup>+Van-treated group (scale bar: 100  $\mu$ m). **(D)** Bar graphs depict MitoSOX red fluorescence intensity in control, MPP<sup>+</sup>, Van, and MPP<sup>+</sup>+Van-treated SH-SY5Y cells. Values are given as mean  $\pm$  SEM ( $n=3$ ), \*\* $p<0.01$  and \*\*\* $p<0.001$  vs. control # $p<0.05$ , ## $p<0.01$  and ### $p<0.001$  vs. MPP<sup>+</sup>-treated groups

cells was significantly ( $p<0.01$ ) higher in MPP<sup>+</sup>-treated cells than in the control cells. When MPP<sup>+</sup> administered SH-SY5Y cells were treated with Van, the percentage of apoptotic cells was significantly ( $p<0.05$ ) reduced. This confirms that Van treatment significantly reduces the MPP<sup>+</sup>-induced apoptosis in SH-SY5Y cells. Compared to MPP<sup>+</sup>-administrated cells, Van treatment significantly reduces the percentage of apoptotic cells by 1.65-fold (Fig. 5C,  $F=13.69$ ,  $p<0.05$ ). According to these findings, Van treatment decreased MPP<sup>+</sup>-induced apoptosis and exerted anti-apoptotic properties in MPP<sup>+</sup>-induced SH-SY5Y cells. The representative Annexin/PI fluorescence images from the control, MPP<sup>+</sup>, Van, and MPP<sup>+</sup>+Van-treated groups are shown in Fig. 5B.

### Van Treatment Improves Gene Dysregulations in SH-SY5Y Cells

The impact of MPP<sup>+</sup> administration and Van treatment on the mRNA expressions of GSK-3 $\beta$ , PARP1 (Poly (ADP-ribose) (PAR) polymerase-1), p53, Bcl-2, Bax, and Caspase-3 in SH-SY5Y cells is shown in Fig. 6. In SH-SY5Y cells, MPP<sup>+</sup> administration significantly ( $p<0.001$ ) elevated the GSK-3 $\beta$  mRNA levels in comparison to the control group. At the same time, the Van treatment significantly reduced the GSK-3 $\beta$  mRNA expression by 1.4-fold compared to the cells treated with MPP<sup>+</sup> (Fig. 6A,  $F=35.10$ ,  $p<0.001$ ). MPP<sup>+</sup>

administration resulted in a significant ( $p<0.01$ ) increase in mRNA levels of PARP1 compared to the control, whereas SH-SY5Y cells treated with Van showed a significant reduction in mRNA levels of PARP1 by 2.4-fold compared to the MPP<sup>+</sup>-treated cells (Fig. 6B,  $F=14.13$ ,  $p<0.001$ ). MPP<sup>+</sup> administration also significantly ( $p<0.001$ ) elevated the mRNA expression of the p53 gene compared to the control, and a 2.19-fold decrease in the mRNA levels of p53 was observed in cells treated with Van in comparison to MPP<sup>+</sup>-treated SH-SY5Y cells (Fig. 6C,  $F=16.52$ ,  $p<0.001$ ). Likewise, the administration of MPP<sup>+</sup> significantly ( $p<0.01$ ) lowered Bcl-2 mRNA levels compared to the control, but Van-treated cells had significantly 2.36-fold enhanced Bcl-2 mRNA levels in comparison to MPP<sup>+</sup>-treated cells (Fig. 6D,  $F=16.09$ ,  $p<0.05$ ). MPP<sup>+</sup> significantly ( $p<0.001$ ) increased Bax mRNA levels in comparison to the control; however, Van treatment significantly ( $p<0.001$ ) suppressed MPP<sup>+</sup>-induced elevated Bax mRNA expressions (Fig. 6E,  $F=20.36$ ,  $p<0.001$ ). MPP<sup>+</sup> administration resulted in a significant ( $p<0.001$ ) increase in Caspase-3 mRNA expressions in SH-SY5Y cells compared to the control. At the same time, the Van treatment led to a significant reduction in Caspase-3 mRNA expressions by 2.3-fold when compared with the MPP<sup>+</sup>-administered group. (Fig. 6F,  $F=9.312$ ,  $p<0.01$ ). These findings indicate that Van provides significant neuroprotection in MPP<sup>+</sup>-induced SH-SY5Y cells by reducing MPP<sup>+</sup>-induced aberrant mRNA expressions of GSK-3 $\beta$ , PARP1, p53, Bcl-2, Bax, and Caspase-3 genes.

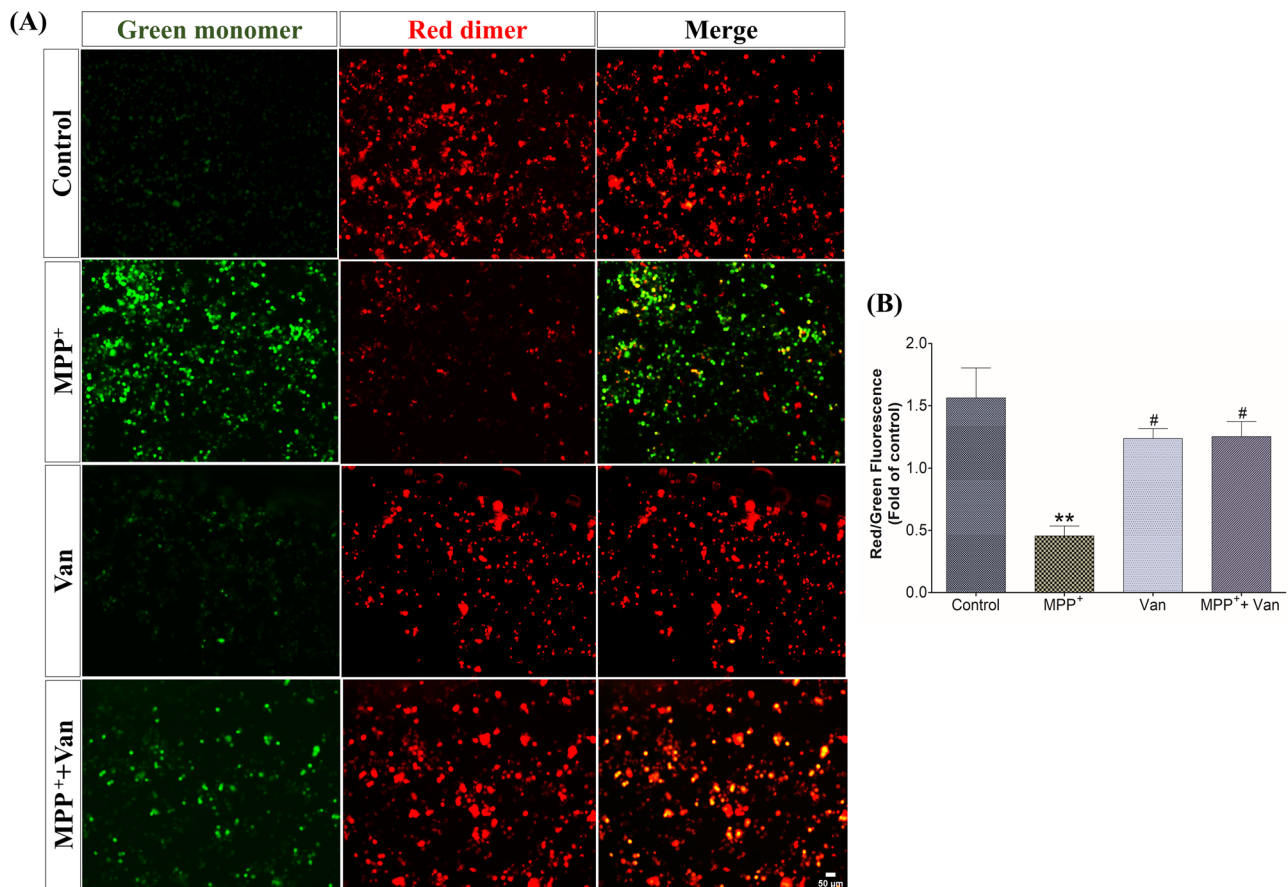


**Fig. 4** Mitochondrial membrane potential depolarization was evaluated by JC-1 staining. **(A)** Fluorescent microscopy images showing the Red/Green JC-1 fluorescence in control, MPP<sup>+</sup>, Van, and MPP<sup>+</sup> + Van-treated group (scale bar: 50  $\mu$ m). **(B)** Bar graph depict-

ing comparative JC-1 Red/Green fluorescence in control, MPP<sup>+</sup>, Van, and MPP<sup>+</sup> + Van-treated groups. Values are given as mean  $\pm$  SEM ( $n=3$ ), \*\* $p < 0.01$ , vs. control and # $p < 0.05$  vs. MPP<sup>+</sup>-treated group

### Van Upregulates TH Protein Expression in SH-SY5Y Cells

To further analyze the MPP<sup>+</sup>-induced cytotoxicity and neuroprotective impact of Van, we assessed the protein expression of TH in SH-SY5Y cells, which is the rate-limiting enzyme in/for dopamine synthesis. Indeed, MPP<sup>+</sup> administration significantly ( $p < 0.001$ ) decreased the TH protein expression in the MPP<sup>+</sup>-treated group in comparison to the control group. Van treatment significantly increased the protein expression of TH by 1.8-fold compared to MPP<sup>+</sup>-treated cells (Fig. 7B,  $F = 47.75$ ,  $p < 0.001$ ). Figure 7A depicts a representative western blot image of TH protein expression in the control, MPP<sup>+</sup>, Van, and MPP<sup>+</sup> + Van-treated groups. Van enhanced TH protein levels, suggesting it can inhibit MPP<sup>+</sup>-induced TH suppression, likely by reducing ROS production and apoptosis.

### Van Alleviates MPTP-Induced Motor Dysfunctions

To determine the neuroprotective ability of Van on MPTP-induced motor dysfunctions in PD mice, the pole test and narrow beam test were conducted at the end of the dosing regime (Fig. 8A). Results showed contrasting comparisons in MPTP-lesioned mice and controls in the pole test (descent time: Fig. 8B,  $F = 213.3$ ,  $p < 0.001$ ) and narrow beam test (average time to cross the beam: Fig. 8C,  $F = 44.29$ ,  $p < 0.001$ ; the number of foot slips: Fig. 8D,  $F = 48.05$ ,  $p < 0.001$ ). MPTP-lesioned mice exhibited apparent motor dysfunctions, took longer time to descend ( $p < 0.001$ ) in the pole test and time to cross the beam compared to the control group ( $p < 0.001$ ), with more foot slips ( $p < 0.001$ ). Results showed a significant reduction in motor impairments such as decreased time to descend the pole, taking lesser time in crossing the beam, and decreased foot slip number in Van ( $p < 0.001$ ,

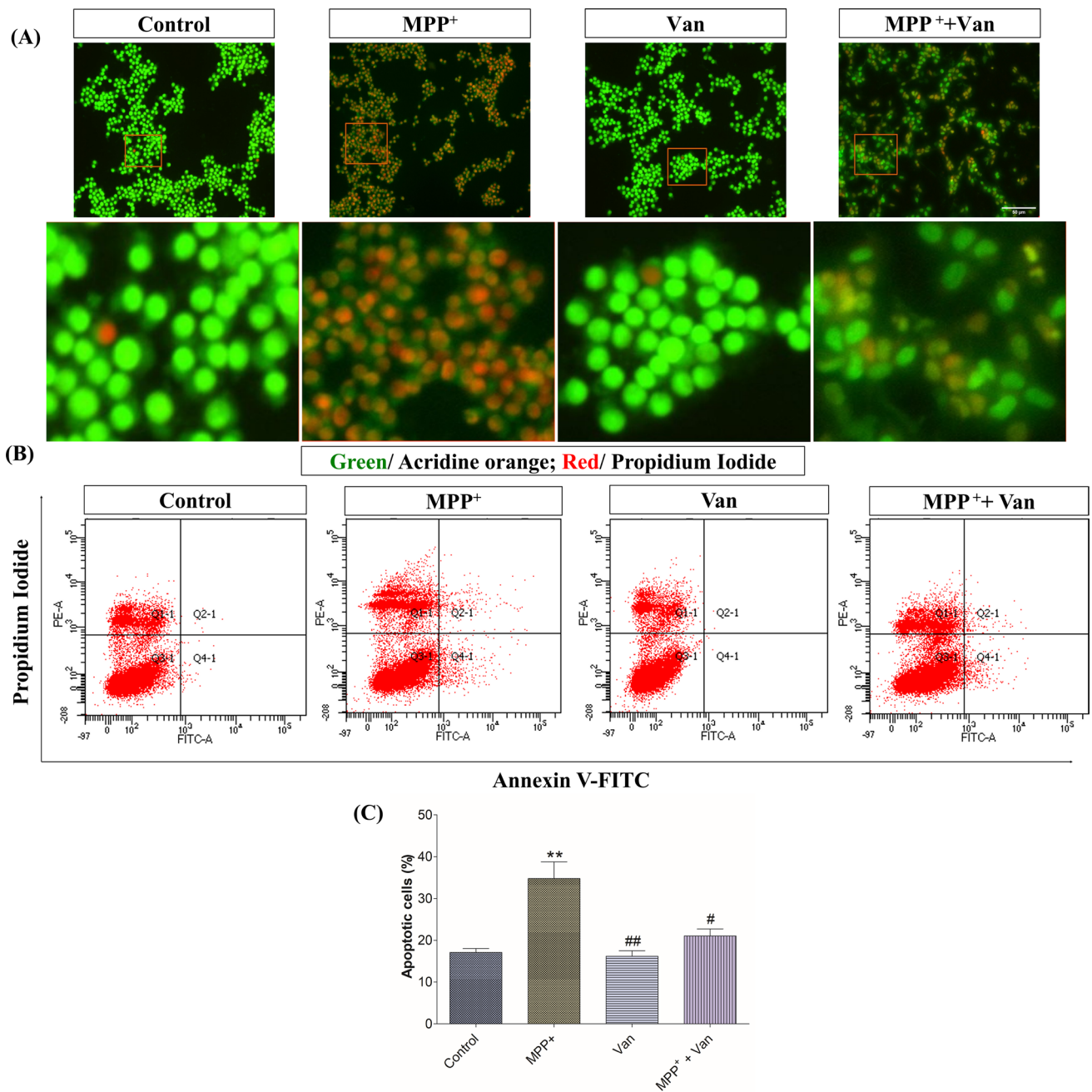


**Fig. 5** Effect of Van on apoptosis in MPP<sup>+</sup>-induced SH-SY5Y cells. **(A)** Representative fluorescence images of AO (green) and PI (red) dual-stained SH-SY5Y cells in control, MPP<sup>+</sup>, Van, and MPP<sup>+</sup> + Van-treated group (scale bar: 50  $\mu$ m). Images were obtained using a fluorescent microscope (Eclipse Ti-E, Nikon) at a scale bar of 50  $\mu$ m. **(B)** Apoptosis of SH-SY5Y cells was evaluated by Annexin-V/PI double

staining in control, MPP<sup>+</sup>, Van, and MPP<sup>+</sup> + Van-treated group. **(C)** Bar graph showing comparative percentage apoptotic cells in control, MPP<sup>+</sup> administered, Van, and MPP<sup>+</sup> + Van-treated SH-SY5Y cells. Values are given as mean  $\pm$  SEM ( $n=3$ ), \*\* $p < 0.01$  vs. control and # $p < 0.05$  and ## $p < 0.01$  vs. MPP<sup>+</sup>-treated groups

$p < 0.01$ ,  $p < 0.001$  respectively), MPTP + Van ( $p < 0.001$ ,  $p < 0.01$ ,  $p < 0.05$  respectively), and MPTP + L-DOPA ( $p < 0.001$ ,  $p < 0.001$ ,  $p < 0.001$  respectively)-treated groups compared to the MPTP-treated mice. These results reflect that Van attenuates MPTP-induced motor dysfunction.

### Van Treatment Did Not Alter Striatal MPP<sup>+</sup> Levels

Since MPTP-induced dopaminergic neurotoxicity relies on the conversion of MPTP to its toxic metabolite MPP<sup>+</sup> in the nigrostriatal pathway, it was crucial to rule out Van affecting MPTP metabolism to MPP<sup>+</sup> in the mice striatal tissues.

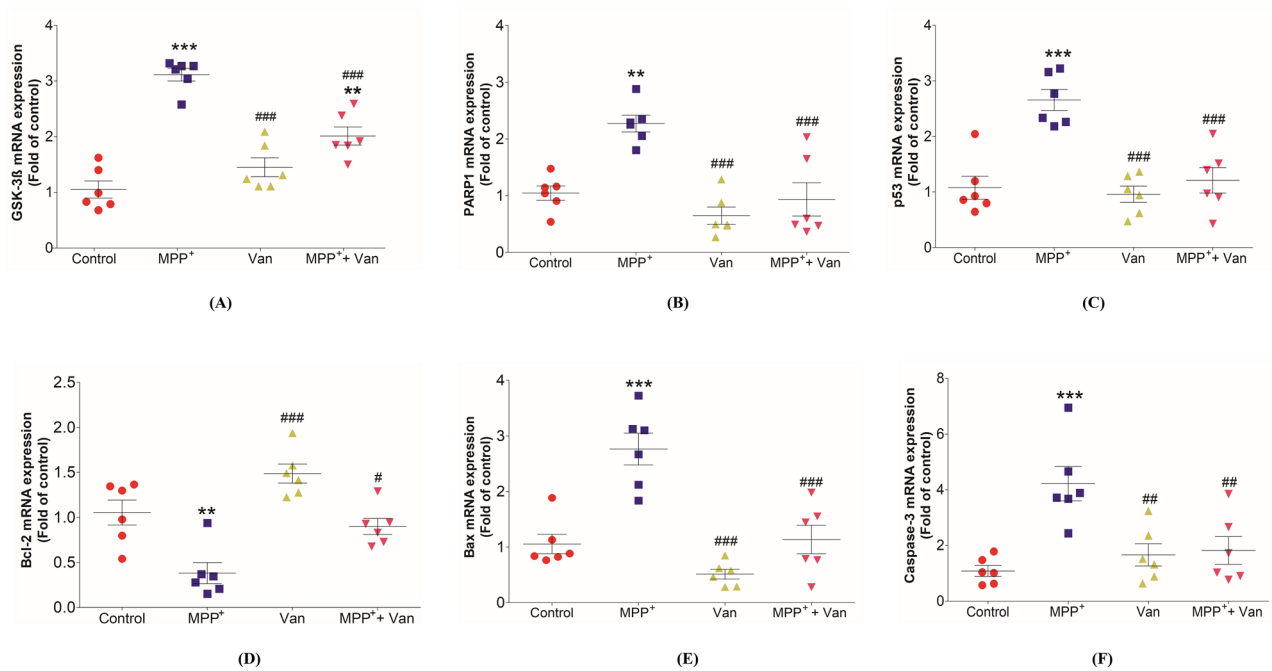


**Fig. 6** Effect of Van on MPP<sup>+</sup>-induced mRNA expression changes: RT-PCR was used to analyse the mRNA expression of (A) GSK-3β, (B) PARP1, (C) p53, (D) Bcl-2, and (E) Bax, and (F) Caspase-3 with

β-actin as a loading control. Values are given as mean ± SEM (*n* = 3), \*\**p* < 0.01 and \*\*\**p* < 0.001 vs. control and #*p* < 0.05, ##*p* < 0.01 and ###*p* < 0.001 vs. MPP<sup>+</sup>-treated group

Thus, we examine the impact of Van on striatal MPP<sup>+</sup> levels using HPLC (Fig. 8E and F). The mice were randomly divided into two groups: MPTP and MPTP + Van. Our results showed no significant changes in the striatal MPP<sup>+</sup> level in MPTP-treated mice with and without Van treatment (MPTP, 22.136 ± 1.009 ng/mg tissue; MPTP + Van group, 19.956 ± 1.453 ng/mg tissue; *p* > 0.05; Fig. 8G). These findings suggest that Van did not alter the MPTP metabolism, as striatal MPP<sup>+</sup> levels in the MPTP group did not differ from those in the MPTP + Van group.

### Van Modulates MPTP-Induced Oxidative Stress Biomarkers

Figure 9 depicts the effects of MPTP and Van treatment on GSH levels, SOD, CAT activity, and LPO content in the striatum of mice. Compared to control and L-DOPA-treated mice, MPTP administration significantly (*p* < 0.001) lowered GSH levels in the striatum. Van treatment significantly increases GSH levels by 1.7-fold more than MPTP-treated mice (Fig. 9A, *F* = 9.179,

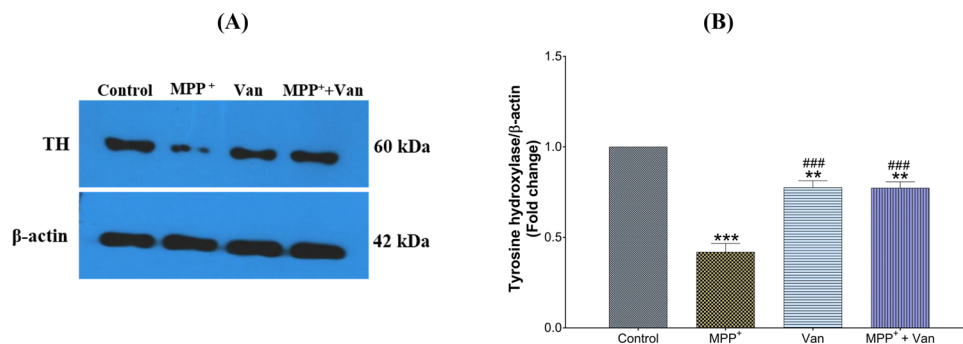


**Fig. 7** The representative western blot image shows the effect of Van treatment on TH protein expression in the MPP<sup>+</sup>-intoxicated SH-SY5Y cells. (B) The bar graph represents comparative TH expression (fold change) in control, MPP<sup>+</sup>, Van, and MPP<sup>+</sup> + Van-treated

groups. Values are given as mean ± SEM. Significant differences are expressed as \*\**p* < 0.01 and \*\*\**p* < 0.001 vs. control and ###*p* < 0.001 vs. MPP<sup>+</sup>-treated groups



$p < 0.05$ ). When mice were administered MPTP, the activity of the SOD ( $p < 0.001$ ) and CAT ( $p < 0.001$ ) enzymes was significantly elevated compared to the control and L-DOPA-treated mice. Treatment with Van resulted in a 1.5-fold reduction in SOD activity (Fig. 9B,  $F = 10.27$ ,  $p < 0.01$ ) and a 1.6-fold decrease in CAT activity (Fig. 9C,  $F = 8.957$ ,  $p < 0.05$ ) as compared to MPTP-administered animals. MPTP also significantly ( $p < 0.001$ ) elevated the levels of LPO when compared to the control and L-DOPA-treated mice, and Van treatment decreased the LPO levels by 1.8-fold than MPTP-treated mice (Fig. 9D,  $F = 22.87$ ,  $p < 0.01$ ). These findings indicate that Van provides neuroprotection against MPTP-induced oxidative stress by modulating antioxidant enzymes and LPO levels.

## Van Increases TH-Positive Neurons in Mice SNpc

Selective dopaminergic neuronal loss in the SNpc is believed to be initiated way before the onset of symptoms in PD. To assess the MPTP-induced dopaminergic neuronal loss in the SNpc and the effect of Van treatment in reducing the neuronal deficits in SNpc, we conducted the immunofluorescence and DAB staining (Fig. 10). Our immunofluorescence results show that the SNpc-specific TH-positive neurons were markedly less in the MPTP-treated mice ( $p < 0.001$ ), and Van was significantly (Fig. 10B,  $F = 34.53$ ,  $p < 0.05$ ) able to rescue the decreased loss of TH-positive neurons by 1.4-fold in SNpc. MPTP considerably reduced TH immunofluorescence in the SNpc, reflecting the loss of dopaminergic neurons. Van treatment significantly restored the reduced TH immunofluorescence indicating Van

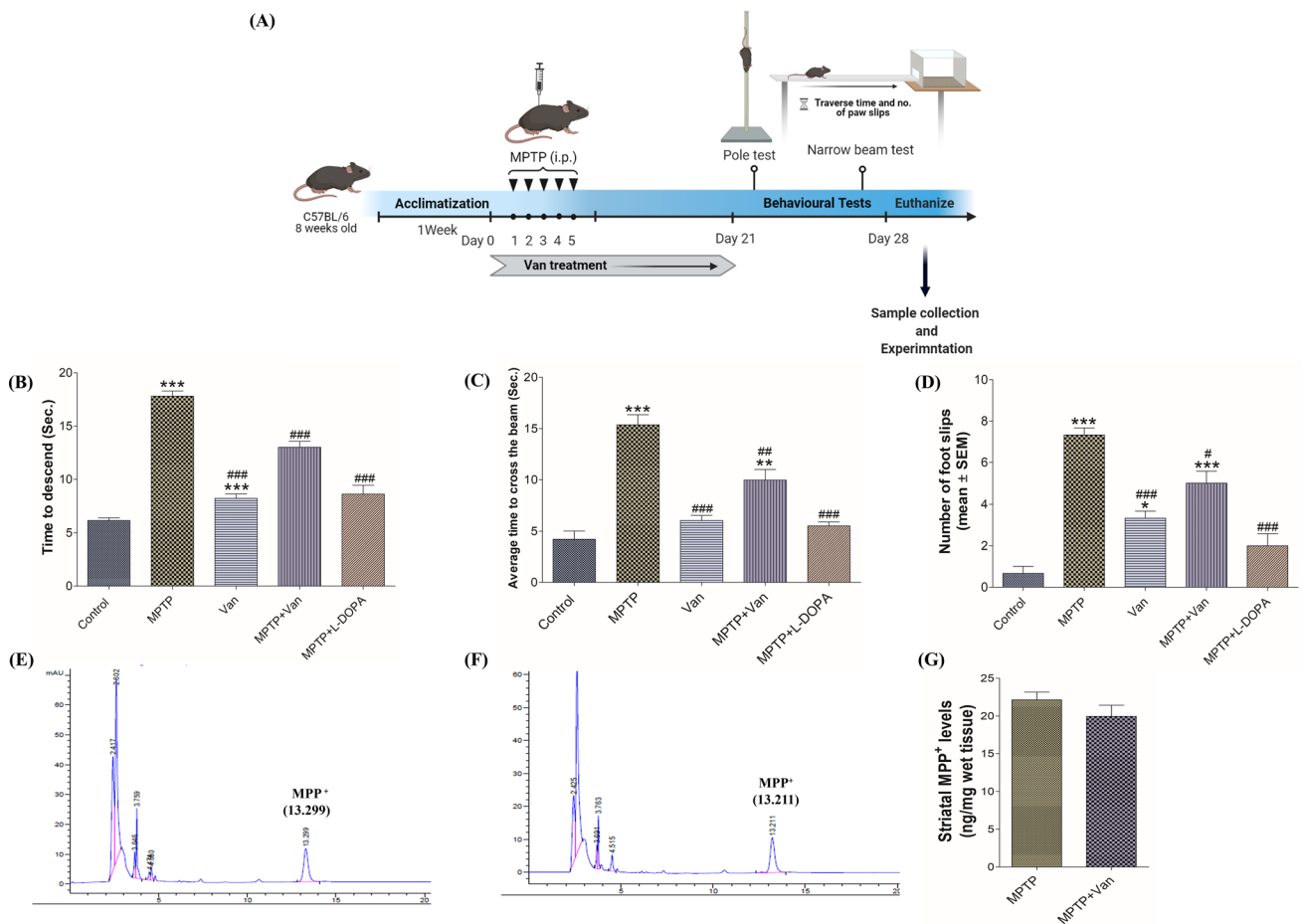


**Fig. 8** Schematic representation of the study design and timeline. **(B)** Graphical representation of the effect of Van treatment on time taken to descend the pole in the pole test. **(C)** Average time to cross the beam in narrow beam test mice after MPTP administration. **(D)** Number of foot slips ( $n=6$ ). **(E, F)** Panels represent typical chromatographs of striatal MPP<sup>+</sup> in MPTP and MPTP+Van-

treated group showing typical retention time for MPP<sup>+</sup> at ~13 min in both groups. **(G)** Bar graphs representing striatal MPP<sup>+</sup> levels in MPTP and MPTP+Van treated group ( $n=4$ ). Values are given as mean  $\pm$  SEM, \* $p < 0.05$ , \*\* $p < 0.01$ , \*\*\* $p < 0.001$  vs. control and # $p < 0.05$ , ## $p < 0.01$ , ### $p < 0.001$  vs. MPTP group



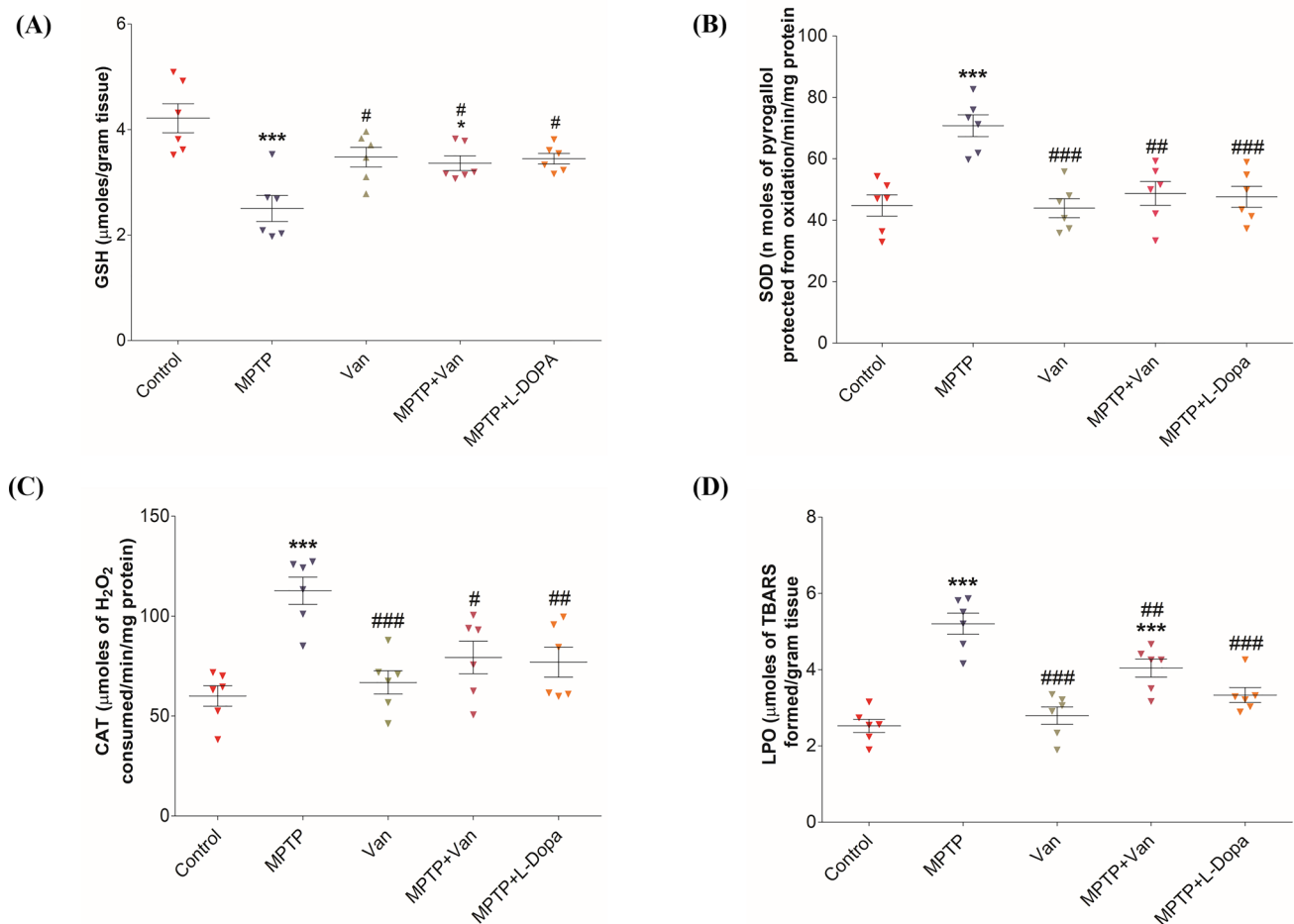


**Fig. 9** Alterations in (A) GSH, (B) SOD activity, (C) CAT activity, and (D) LPO levels following MPTP administration and Van treatment in the mice striatum. Values are given as mean  $\pm$  SEM ( $n=6$ ),

\* $p < 0.05$  and \*\*\* $p < 0.001$  vs. control and # $p < 0.05$ , ## $p < 0.01$  ### $p < 0.001$  vs. MPTP group

protects against MPTP-induced dysregulations in the immunoreactivity of the TH enzyme. Similar to our immunofluorescence, DAB results show that TH-positive neurons in SNpc reduced significantly (Fig. 10D,  $F=27.78$ ,  $p < 0.001$ ) in MPTP-treated mice compared to controls, and Van treatment significantly ( $p < 0.01$ ) increased TH-positive neurons in mice SNpc by 1.5-fold compared to MPTP-treated group. Figure 10A and C depict representative images of immunofluorescence and DAB staining of TH in the SNpc of control, MPTP, Van, MPTP + Van, and MPTP + L-DOPA-treated groups. These data show that Van treatment protects against MPTP-induced dopaminergic neuron loss in the mice SNpc by increasing the number of TH-positive neurons.

### Van Increases the Density of TH-Fibers in Mice Striatum

The nigral fibers ascend along the dorsomedial border of the SNpc. These nigral fibers innervate the striatum. Any

neurodegeneration in SNpc may result in the denervation of dopaminergic terminals in the striatum. Since Van treatment decreased the loss of TH-positive neurons in SNpc induced by MPTP administration, we determined whether Van treatment could also upregulate TH-fibers in the mice striatum by conducting DAB staining (Fig. 11). Our results show that MPTP administration resulted in a significant ( $p < 0.001$ ) reduction in the levels of TH-fibers in the striatum of mice brain than the control, and Van treatment was significantly (Fig. 11B,  $F=14.68$ ,  $p < 0.05$ ) able to increase the number of TH-fibers by 2.1-fold compared to MPTP-lesioned mice striatum. Similar to an increase in TH in cell bodies of SNpc by Van treatment, our results show the increased density of TH-fibers in the striatal tissues of Van-treated mice compared to MPTP-administered mice. Figure 11A depicts representative images of TH-fibers in mice striatum of the control, MPTP, Van, and MPTP + Van, and MPTP + L-DOPA-treated groups. Taken together, our immunofluorescence and DAB staining results indicate that Van

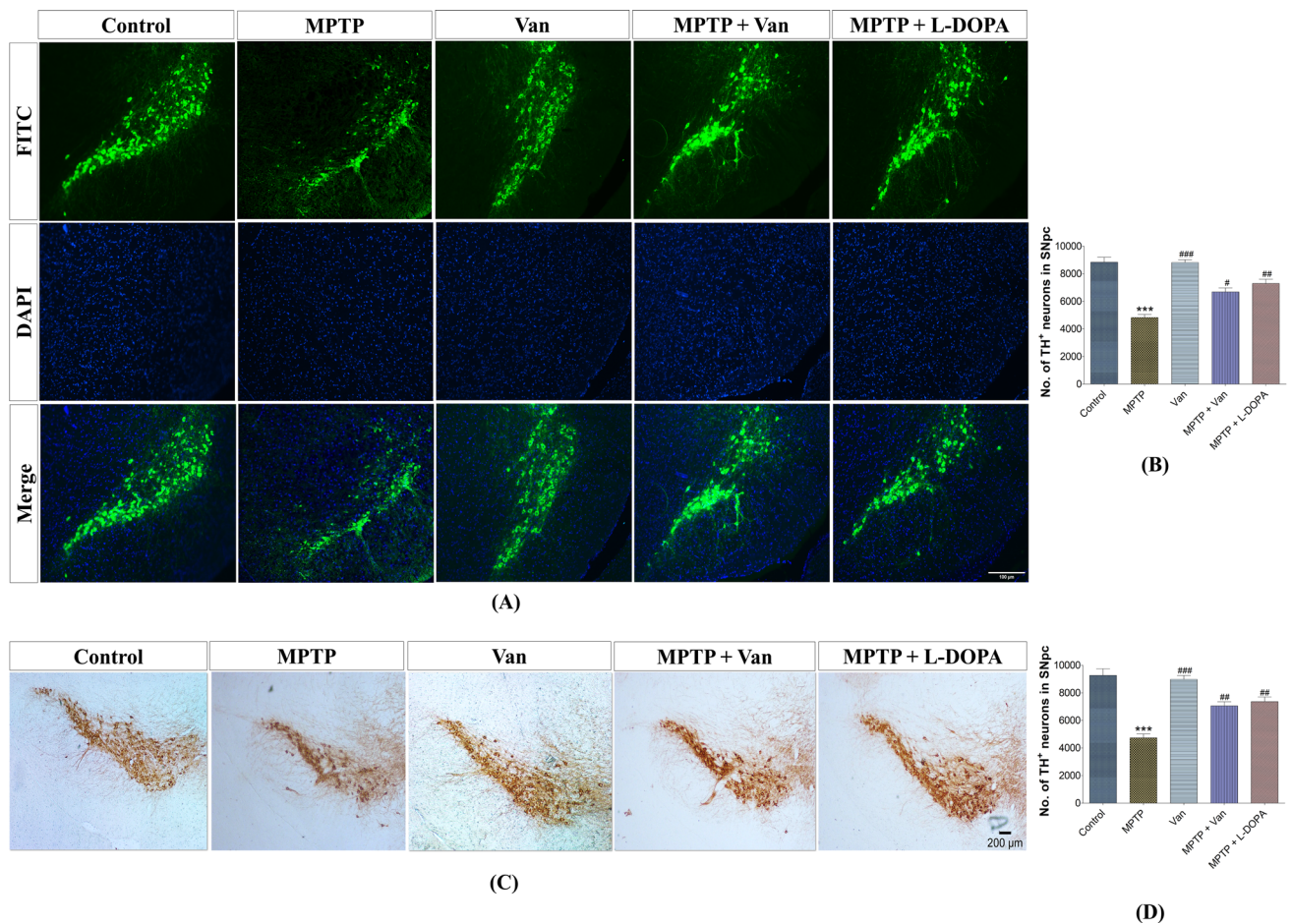


**Fig. 10** Effect of MPTP administration and Van treatment on the level of TH-positive neurons in the SNpc of mice brain. **(A and C)** Representative images of TH immunofluorescence and DAB staining in control, MPTP, Van, MPTP+Van, and MPTP+L-DOPA (immunofluorescence scale bar:100 μm; DAB staining scale bar:

200 μm). **(B and D)** Bar graphs depict the comparative no. of TH-positive neurons in SNpc of control, MPTP, Van, MPTP+Van, and MPTP+L-DOPA-treated groups. Values are given as mean ± SEM (n=4); \*\*\*p < 0.001 vs. controls and #p < 0.05, ##p < 0.01, and ####p < 0.001 vs. MPTP groups

treatment reduces MPTP-induced dopaminergic neuronal loss in the mice SNpc and striatum.

### Van Modulates MPTP-Induced Neuro Histopathological Alterations

The total number of neurons in the SNpc was estimated to investigate whether MPTP administration caused only the reduction in TH expression or the actual loss of the TH and Nissl-positive cells. Figure 12A and B depict the estimated number of Nissl-stained cells in the SNpc of each of the five experimental groups. The overall number of Nissl-positive cells in control and Van group was relatively similar (Fig. 12B,  $F = 17.57$ ). The number of Nissl-stained cells was reduced by 1.7-fold in the MPTP group compared to that in the control and Van-treated groups. The number of Nissl-positive cells in the MPTP + Van group was almost equal to the number of cells in the control and

Van groups. The MPTP + Van group showed 1.3-fold more Nissl-stained cells in the SNpc than in the MPTP group. Using the multiple comparison test, it was determined that there were significant differences in the number of Nissl-positive cells between the MPTP control ( $p < 0.001$ ), Van ( $p < 0.001$ ), and MPTP + Van ( $p < 0.05$ ) groups. Compared to the control and Van groups, the MPTP group showed 1.7-fold reductions in Nissl-stained cells. The number of Nissl-positive cells in the MPTP + Van group were similar to those of the controls and 1.3-fold higher than those of the MPTP group. These results demonstrated that Van treatment protected SNpc cells from MPTP intoxication apart from inhibiting the downregulation of TH expression in dopaminergic neurons.

MPTP treatment also caused vacuolar degeneration and induced pyknotic nuclei in the striatum of mice. The control mice did not show any neurodegeneration phenotypically and exhibited neurons containing normal nuclei.

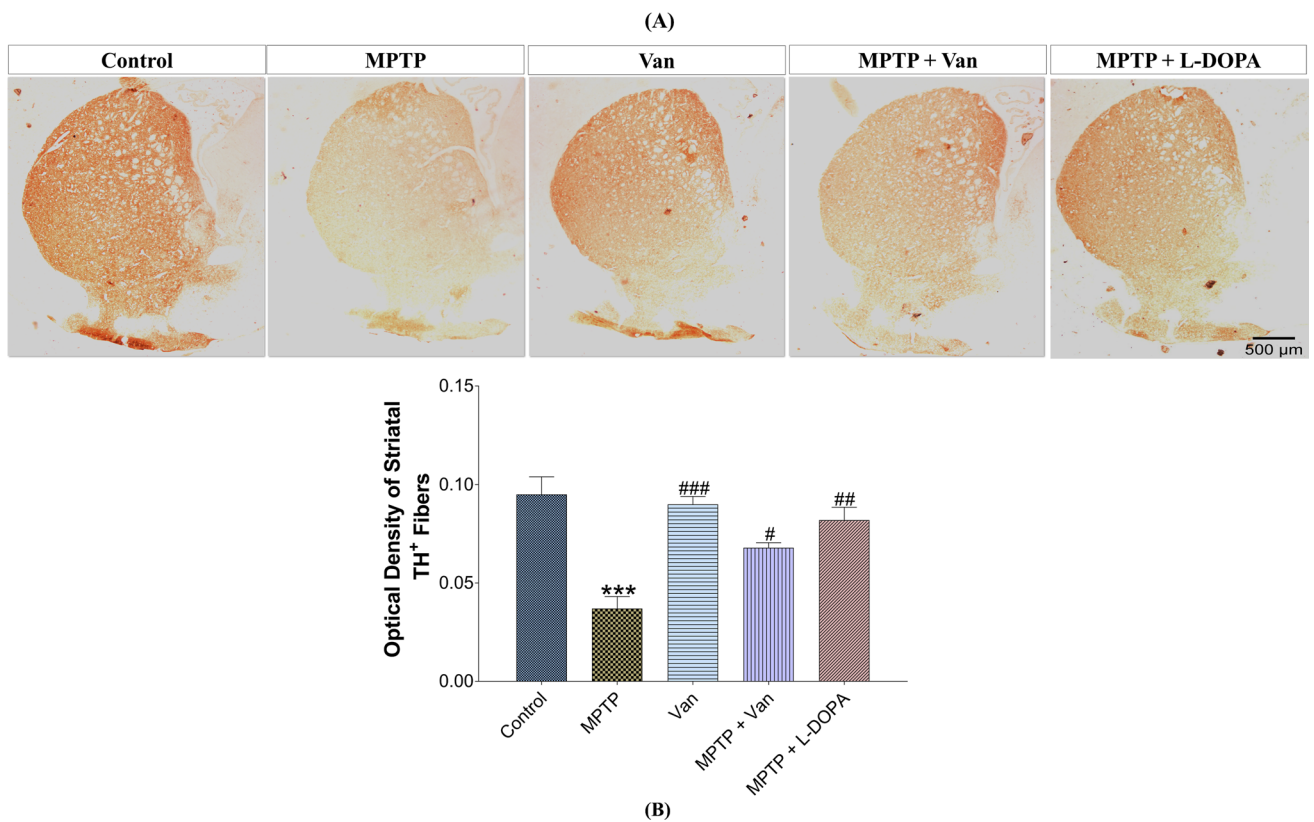


**Fig. 11** Effect of MPTP administration and Van treatment on the TH-fiber density in mice striatum. (A) Representative DAB images of TH in control, MPTP, Van, MPTP + Van, and MPTP + L-DOPA (scale bar: 500 μm). (B) Bar graph showing the relative density of

TH-fibers in the striatum of control, MPTP, Van, MPTP + Van, and MPTP + L-DOPA-treated groups. Values are given as mean ± SEM ( $n=4$ ), \*\*\* $p < 0.001$  vs. control and # $p < 0.05$ , ## $p < 0.01$ , and ### $p < 0.001$  vs. MPTP group

However, treatment with Van significantly decreased histopathological alterations in comparison to MPTP + Van and MPTP + L-DOPA-treated mice. Our data suggest that Van protects against MPTP-induced toxicity (Fig. 12C).

### Discussion

PD pathogenesis is primarily associated with dopaminergic neuronal death in the nigrostriatal pathway. The cause

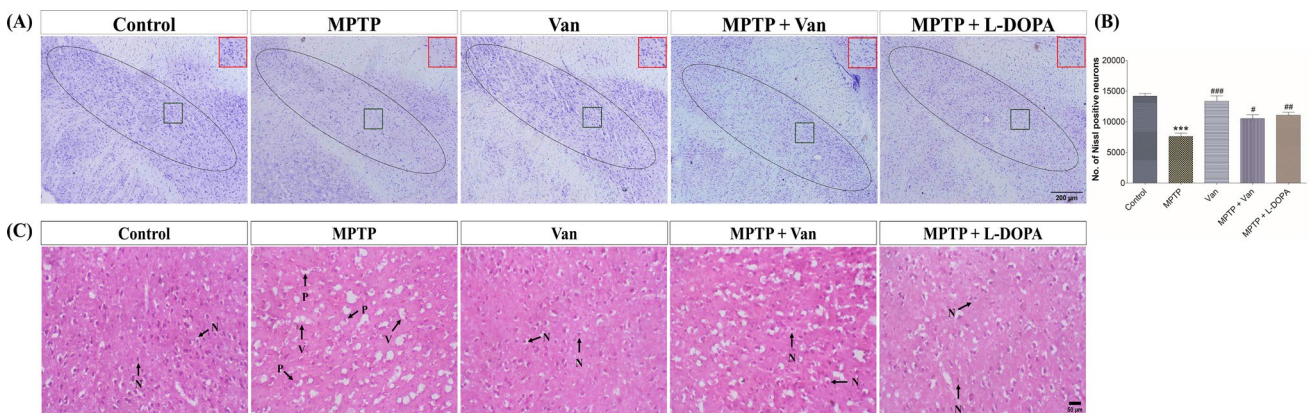


**Fig. 12** Effect of Van on MPTP-induced histopathological alterations. (A) Photomicrographs of Nissl-stained neurons in mice SNpc (scale bar: 200 μm). (B) Bar graph depicting comparative no. of Nissl positive neurons in SNpc of control, MPTP, Van, MPTP + Van, and MPTP + L-DOPA-treated groups. Values are given as mean ± SEM

( $n=4$ ), \*\*\* $p < 0.001$  vs. controls and # $p < 0.05$ , ## $p < 0.01$ , and ### $p < 0.001$  vs. MPTP groups. (C) Photomicrographs of H&E-stained coronal sections from mice striatum showing histopathological alterations (scale bar: 50 μm), neurons with vacuolar degeneration (V); normal nuclei (N); and Pyknotic nuclei (P)



of dopaminergic loss in PD is unclear, but about 90% of the sporadic PD cases have been associated with exposure to environmental toxins like MPTP [37]. Oxidative stress appears to be a central event related to the pathogenesis of PD, and MPTP has been reported to induce oxidative stress by either acting singly or in concert, resulting in dopaminergic neuronal death in the SNpc and striatum [10]. MPP<sup>+</sup>/MPTP is a neurotoxic compound that selectively targets dopaminergic neurons in basal ganglia and causes irreversible Parkinsonism-like symptoms. MPP<sup>+</sup>/MPTP has been extensively used to investigate the neurodegenerative implications that might occur in PD. Because of their diverse pharmacological activities as an anti-oxidant, anti-inflammatory, and neuroprotective properties, and their ability to combat oxidative stress, diet-derived phenolic compounds have been considered as alternatives for treating neurodegenerative diseases, including PD [38]. One such phenolic flavonoid, Van, exhibits neuroprotection against PD pathology in different animal models [17, 39]. The present study, therefore, explored the potential neuroprotective of Van on MPP<sup>+</sup>/MPTP-induced Parkinsonism in SH-SY5Y cells and a mouse model of PD. In the current study, SH-SY5Y cells were used because of being more susceptible to MPP<sup>+</sup>-induced cytotoxicity and have TH and dopamine- $\beta$ -hydroxylase activities [40], and for in vivo experiments, we used C57BL/6 mice for being the most sensitive to MPTP intoxication compared to other rodent models [10]. Our results showed that Van treatment did not alter MPTP metabolism, as the striatal MPP<sup>+</sup> levels in the MPTP group did not differ from those in the MPTP + Van group. To our best knowledge, this study is the first to demonstrate the effect of Van on mice striatal MPP<sup>+</sup> levels. The observed neuroprotective effect of Van against MPTP-induced neurotoxicity in our experiments was not due to alterations in MPTP metabolism but rather Van inhibiting the MPTP-induced oxidative stress in the nigrostriatal pathway. In our study, the administration of MPP<sup>+</sup> resulted in a loss of cell viability in SH-SY5Y in a concentration-dependent manner, consistent with an earlier study [41]. However, in agreement with previous reports, Van at different concentrations negated the MPP<sup>+</sup>-induced loss in cell viability and improved survival in RA-mediated differentiated SH-SY5Y cells [42]. MPTP rapidly crosses the blood–brain barrier and is converted to MPP<sup>+</sup> in astrocytes by the enzyme MAO-B [10]. MPP<sup>+</sup> then enters into the dopaminergic neurons via the DAT and accumulates in the mitochondria, where it causes the excessive generation of ROS by inhibiting the mitochondrial respiratory complex I [43]. Similar to our results, a recent study reported that MPP<sup>+</sup> caused significant intracellular ROS generation in SH-SY5Y cells [44]. In the present study, Van treatment ameliorated the MPP<sup>+</sup>-induced generation of excess ROS in SH-SY5Y cells. Our findings are in line with previous findings where Van treatment inhibited the generation of ROS

in rotenone-administered SH-SY5Y human neuroblastoma cells [21] and caused a significant reduction in ROS production in undifferentiated SH-SY5Y cells [45]. Our in vivo results from the mouse model also reflect that Van treatment significantly alleviated the MPTP-induced oxidative stress by modulating the alterations of antioxidant status: SOD and CAT activities, GSH content, and LPO levels. These observations are again in line with the previous study in which Van modulated maneb-induced oxidative stress in Swiss albino mice [18, 46]. Our results and these observations are further corroborated by a recent finding where Van and vanillic acid modulated antioxidant defense systems in brain tissue damage [47]. In the present study, the Van-mediated inhibition in ROS generation may be attributed to its free radical scavenging property and its ability to undergo separate acetylation and reduction by donating electrons or hydrogen atoms and converting 1, 1-diphenyl-2-picrylhydrazyl (DPPH) radical to non-radical form; 1, 1-diphenyl-2-picryl hydrazine [48].

Clinically, PD is characterized by motor deficits, and reports suggest MPTP is implicated in neurobehavioral impairments during the progression of PD, which may be attributed to a significant loss of SNpc neurons and dysfunctions in nigrostriatal dopamine circuits [49]. A recent study reported that MPTP induced motor deficits and dopaminergic neurodegeneration in C57BL/6 mice, very much similar to our results where MPTP elevated motor disturbances and caused degeneration of dopaminergic neurons [50]. Van has recently been reported to alleviate tremors (early motor deficits in PD) in rats induced by harmaline, a  $\beta$ -carboline alkaloid and structural analog of MPTP [51]. Another study also confirmed these observations in which rotenone-induced behavioral disorders were attenuated by Van in a rat model of PD [19]. In agreement with observations, our results also demonstrate that Van successfully alleviated the MPTP-induced motor dysfunction, which may be due to the Van-mediated amelioration of oxidative stress and preserving striatal dopamine levels [19].

MPP<sup>+</sup>-induced oxidative stress may partly disrupt the mitochondrial permeability transition pore, altering the  $\Delta\psi_m$ . Increased mitochondrial ROS may cause  $\alpha$ -synuclein accumulation and aggregation, followed by proteasomal dysfunction, making the mitochondrial transmembrane more permeable, releasing cytochrome-c and activating Caspase-3 resulting in neuronal cell death during PD pathology [4]. Mitochondria are the key source of MPP<sup>+</sup>-induced ROS production in the brain. MPP<sup>+</sup> enters dopaminergic neurons, accumulates in the mitochondria, and alters the  $\Delta\psi_m$ . MPP<sup>+</sup> causes mitochondrial aberrations by increasing oxidative stress and altering  $\Delta\psi_m$  [52]. These observations are consistent with our results, where MPP<sup>+</sup> dysregulated mitochondrial function by altering the  $\Delta\psi_m$  in SH-SY5Y cells. In the current study, Van treatment effectively reduced

the MPP<sup>+</sup>-induced aberrant mitochondrial activity by restoring  $\Delta\psi_m$ . The results of the present study are in line with the previous report, where Van inhibited the depolarization of  $\Delta\psi_m$  in SH-SY5Y cells [45]. Another study also confirmed these observations in which rotenone administration depolarizes  $\Delta\psi_m$  in SH-SY5Y cells, and Van treatment prevented this by ameliorating the rotenone-induced disruption of  $\Delta\psi_m$  in the in vitro model of PD [21]. Thus, consistent with other studies, the current study shows that Van treatment successfully modulates the MPP<sup>+</sup>-induced aberrations in  $\Delta\psi_m$  in the cellular model of PD.

The pathophysiology of PD is also characterized by aberrant transcription of genes responsible for cellular proliferation, fate determination, and neuronal differentiation [53]. An increase in oxidative stress causes impairment of redox signaling and intracellular signaling pathways. Our findings show that MPP<sup>+</sup> causes dysregulations in gene expression and that Van treatment may be able to regulate these MPP<sup>+</sup>-induced transcriptional aberrations. GSK-3 $\beta$  is the keystone protein involved in many of the multidirectional signaling pathways, and reports suggest its activation/dysregulations induce loss of dopaminergic neurons in PD [54]. It has been demonstrated that GSK-3 $\beta$  dysregulation results in aberrant mitochondrial activity, which is linked to the etiology of PD [55]. GSK-3 $\beta$ -mediated phosphorylation of substrates such as  $\alpha$ -synuclein can result in intracellular and axonal deposits that may be involved in GSK-3 $\beta$ -mediated PD pathogenesis [56]. GSK-3 $\beta$  inhibition has been proposed as a possible therapeutic approach for the treatment of PD. Previous studies have demonstrated high expression of GSK3 $\beta$  in MPP<sup>+</sup>-intoxicated SH-SY5Y cells, which are corroborated with the MPP<sup>+</sup>-induced elevated mRNA expressions of GSK-3 $\beta$  in SH-SY5Y cells in the present findings [57]. In this study, Van treatment protected dopaminergic neurons against MPP<sup>+</sup>-induced GSK-3 $\beta$  activation by reducing mRNA expression of GSK-3 $\beta$  in SH-SY5Y cells. These observations agree with a previous report in which the Van derivative modulates GSK-3 $\beta$ /Wnt/ $\beta$ -catenin signaling [58]. PARP1 is a ribozyme that helps cell survival by recognizing and repairing DNA damage [59]. DNA damage results in the over-activation of the enzyme PARP-1, resulting in the pathogenesis of AD and PD [60]. It has been shown that PARP1 may be stimulated by aggregated  $\alpha$ -synuclein, and this mechanism exacerbates  $\alpha$ -synuclein toxicity. Recently, it has been demonstrated that PARP1 inhibition appears to be a potential and possible strategy for PD [61]. PARP1 activation also disrupts mitochondrial function by altering NAD<sup>+</sup> levels and energy consumption, followed by PARylation-induced depolarization of mitochondrial membrane potential [62]. Earlier findings show that MPP<sup>+</sup> induced neuronal death by upregulating apoptotic signaling in cleaved PARP in SH-SY5Y cells, which is consistent with present results where MPP<sup>+</sup> resulted in the over-expression of PARP1 gene

[63]. In agreement with a previous study, Van treatment modulated the MPP<sup>+</sup>-induced aberrant transcription activation of PARP1 [64].

In the mitochondrial apoptotic pathway, the interplay between pro-apoptotic and anti-apoptotic proteins regulates the  $\Delta\psi_m$ , and the imbalance between them is critical for the permeabilization of the outer membrane of mitochondria and apoptosis [65]. Overexpression and subcellular translocation of p53 are critical in mitochondrial apoptosis and consequent neurodegeneration. In response to cellular stress, activated p53 interacts with Bcl-2/Bcl-xL and releases Bax/Bak (Bcl-2 antagonist/killer) to open mitochondrial membrane transition pore, resulting in the release of cytochrome c from the mitochondria into the cytosol and stimulates mitochondrial intrinsic apoptotic pathway [66]. Dysregulations in gene expressions of p53 and the Bcl-2/Bax ratio have been reported to be implicated in the pathogenesis of PD [67]. Our results show that MPP<sup>+</sup> administration in SH-SY5Y cells activates mRNA expression of p53, Bax, Bcl-2, and Caspase-3; and these observations suggest that Bax, Bcl-2, Caspase-3-like proteases may play crucial roles in MPP<sup>+</sup>-induced neuronal death, which is in agreement with previous studies [68]. Our results show that Van mitigated the adverse effect of MPP<sup>+</sup> on the expressions of Bax and Bcl-2 via inhibiting p53 mRNA expressions, which is consistent with a previous study where Van prevented rotenone-induced apoptosis by downregulating the expressions of Bax and Caspases and increasing the expression of Bcl-2 [19]. In congruence with these observations and our results, a recent study also reported that vanillin exhibited neuroprotective properties by inhibiting apoptosis in spinal cord injury rat model [68]. In addition, another recent study too reported that Van showed potential protective effects by preventing apoptosis in rats [64]. The inhibition of apoptosis by Van in the present study may be due to its ability to activate antioxidant defense machinery and inhibit oxidative stress.

The TH enzyme is a rate-limiting enzyme in the synthesis of dopamine, and its deficiency has been reported to reduce dopamine function in PD [69]. MPP<sup>+</sup> inactivates the TH enzyme, which may be due to MPP<sup>+</sup>-mediated over-production of proximites, resulting in nitration of the tyrosine residue in TH and loss of enzymatic activity and TH neurons [70]. These observations agree with our results, where MPP<sup>+</sup> administration reduced protein expressions of TH. Cocoa beans improved mitochondrial biogenesis and dopaminergic functions by increasing TH expression in MPP<sup>+</sup>-intoxicated SH-SY5Y cells [71]. Our results corroborate these findings where Van treatment elevated the protein expressions of TH in MPP<sup>+</sup>-intoxicated human neuroblastoma SH-SY5Y cells. Van also increases the number of TH-positive neurons in MPTP-treated mice, suggesting that Van can counteract MPTP-induced TH suppression, presumably by reducing ROS exacerbation.

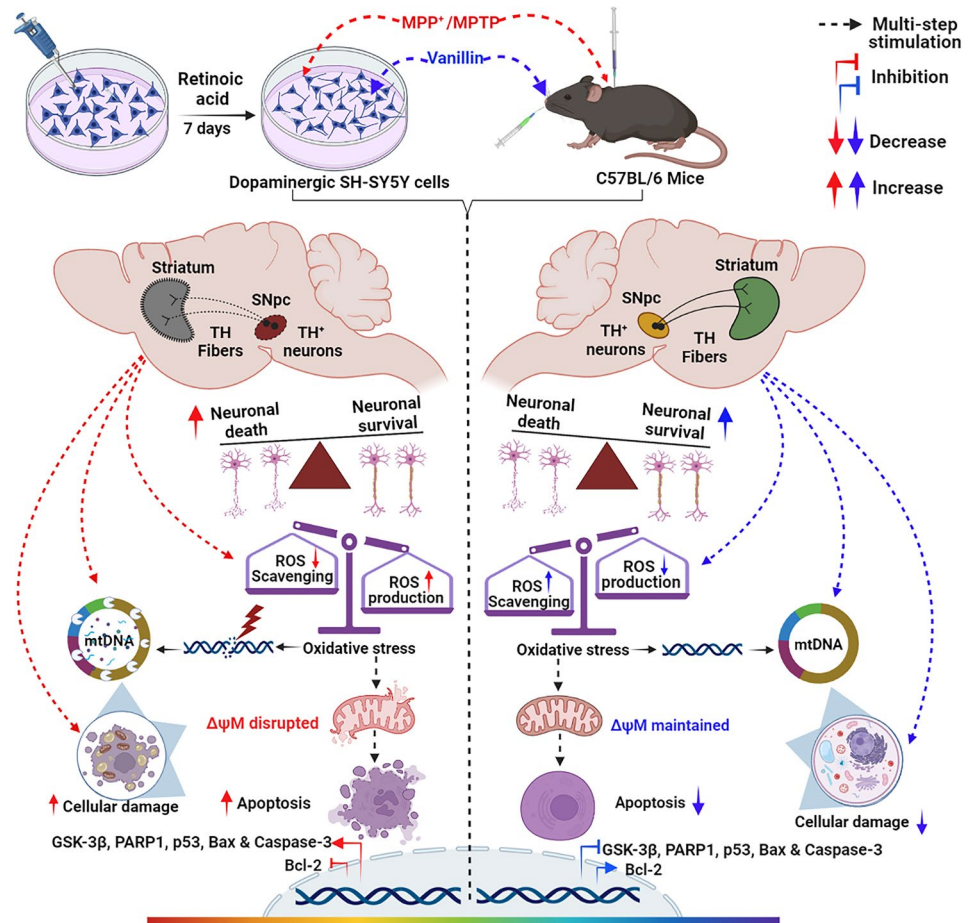


The dysregulations in dopaminergic neurotransmission between the SNpc and the dorsal striatum, known as the nigrostriatal pathway, lower the dopamine levels resulting in motor dysfunctions that characterize PD. This nigrostriatal dopaminergic neurotransmission could be regulated by the level of TH-positive neurons in SNpc and the density of TH-fibers in the striatum. The deregulations in TH expressions mediated by the degeneration of dopaminergic neurons have been implicated in decreasing dopamine levels and manifestations of clinical motor symptoms in PD. They, therefore, reflect the severity and progression of PD. In adult SNpc and striatal neurons, the levels of TH expressions are downregulated in cells that survive exposure to neurotoxins like MPTP [72]. These observations are reflected by our findings showing that MPTP caused degeneration of dopaminergic neurons by increasing the loss of TH-positive neuronal cells and fibers in the mice SNpc and striatum, respectively. Van treatment improved dopaminergic functions by increasing the TH expressions. In line with our findings, Van administration markedly inhibited LPS-induced death of dopaminergic neurons by increasing the number of TH-positive neurons and expression of TH in SNpc of rats [39]. Our observations

indicate that Van-mediated neuroprotection is mediated by its ability to regulate the number and expressions of the TH enzyme. Therefore, our study demonstrates that Van may be a therapeutic approach in the early onset/stage of PD when dopaminergic neurons are still significantly present. Our results show that Nissl-positive neurons in the SNpc were also significantly reduced in MPTP-lesioned mice, which is consistent with previous reports [73, 74] and subsequently, the number of Nissl-positive cells was restored by the Van treatment. Also, there was an increase in the number of TH and Nissl-positive neurons in MPTP-treated mice following Van treatment, suggesting that Van treatment increased the number of dopaminergic neurons in the SNpc.

In conclusion, the present study indicates that Van provides neuroprotection against MPP<sup>+</sup>/MPTP in SH-SY5Y cells and mouse model respectively. It protects against MPP<sup>+</sup> and MPTP-induced degeneration of dopaminergic neurons by alleviating the neurobehavioral impairments, oxidative stress,  $\Delta\psi_m$ , neuronal apoptosis, and gene dysregulations which may be due to Van-mediated improvement in net nigrostriatal TH expressions, i.e., a product of the TH content of SNpc neurons

**Fig. 13** Schematic illustration of the probable mechanism of Van-mediated neuroprotection against MPP<sup>+</sup>/MPTP induced oxidative stress,  $\Delta\psi_m$  perturbations, apoptosis, and aberrant gene and TH expression in SH-SY5Y cells and PD mice model. Created by Bio render



and striatum TH-fibers. Thus, Van may be beneficial for preventing or reducing neuronal loss in the nigrostriatal pathway. Although further investigations about the detailed Van-mediated neuroprotection are required before conclusions can be drawn, our results suggest that Van can be a promising alternative therapeutic approach for preventing and treating PD. The mechanisms of the neuroprotective potential of Van may be because of its ability to protect mitochondrial function and attenuate the generation of intracellular ROS and its potential to inhibit the MPP<sup>+</sup>-induced mitochondrial apoptotic pathway by decreasing the ratio of Bax to Bcl-2, inhibiting the activation of Caspase-3, and by elevating the expression of TH enzyme given in Fig. 13.

**Acknowledgements** The authors would like to acknowledge the Central instrumentation facility, School of Life Sciences, Jawaharlal Nehru University, New Delhi, India. We are grateful to Prof. Ashis K. Nandi, School of Life Sciences, JNU, for his assistance in measuring the striatal MPP<sup>+</sup> levels using HPLC.

**Author Contribution** LR and MHA together designed and performed the experiments, helped analyze the results, and wrote and reviewed the manuscript. BG revised the manuscript. ACM conceptualized, supervised the study, and revised the manuscript. All authors read and approved the final manuscript.

**Funding** This study was partially supported by a grant from DBT (BT/PR32907/MED/122/227/2019), DBT-SAHAJ/BUILDER (BT/INF/22/SP45382/2022) National Facility/Laboratory and DST-FIST-II [(SR/FST/LSII-046/2016(C)) to the School of Life Sciences, JNU. LR and MHA received financial grants from CSIR No. [09/263(1163)/2018-EMR-I] and ICMR (45/7/ 2019/MP/BMS), respectively.

**Data Availability** All data generated or analyzed during this study are included.

## Declarations

**Ethics Approval** All the experiments were carried out on C57BL/6 mice following standard guidelines and regulations of the Institutional Animal Ethics Committee (IAEC), Jawaharlal Nehru University (JNU), New Delhi (10/GO/ReBi/99/CPCSEA/March 10, 1999). All the standard methods and protocols were followed for animal handling and experiments. All efforts were made to reduce animal suffering.

**Consent to Participate** Not applicable.

**Consent for Publication** All authors of the manuscript have agreed to publish this article.

**Competing Interests** The authors declare no competing interests.

## References

- Dorsey ER, Sherer T, Okun MS, Bloem BR (2018) The emerging evidence of the Parkinson pandemic. *J Parkinson's Dis* 8:S3–S8
- Rizek P, Kumar N, Jog MS (2016) An update on the diagnosis and treatment of Parkinson disease. *CMAJ* 188:1157–1165
- Del Rey NL-G, Quiroga-Varela A, Garbayo E, et al. Advances in Parkinson's disease: 200 years later. *Frontiers in Neuroanatomy* 2018;12:113.
- Grünewald A, Kumar KR, Sue CM (2019) New insights into the complex role of mitochondria in Parkinson's disease. *Prog Neurobiol* 177:73–93
- Zhu Y, Zhang J, Zeng Y (2012) Overview of tyrosine hydroxylase in Parkinson's disease. *CNS Neurol Disord: Drug Targets* 11:350–358
- Shehadeh J, Double KL, Murphy KE, et al. Expression of tyrosine hydroxylase isoforms and phosphorylation at serine 40 in the human nigrostriatal system in Parkinson's disease. 2019;130:104524.
- Nagatsu T, Nakashima A, Ichinose H, Kobayashi KJ. Human tyrosine hydroxylase in Parkinson's disease and in related disorders. 2019;126:397-409
- Chia SJ, Tan E-K, Chao Y-X (2020) Historical perspective: models of Parkinson's disease. *Int J Mol Sci* 21:2464
- Meredith GE, Rademacher DJ (2011) MPTP mouse models of Parkinson's disease: an update. *J Parkinsons Dis* 1:19–33
- Mustapha M, Mat Taib CN (2021) MPTP-induced mouse model of Parkinson's disease: a promising direction of therapeutic strategies. *Bosn J Basic Med Sci* 21:422–433
- Sun M-F, Zhu Y-L, Zhou Z-L, et al. Neuroprotective effects of fecal microbiota transplantation on MPTP-induced Parkinson's disease mice: gut microbiota, glial reaction and TLR4/TNF- $\alpha$  signaling pathway. 2018;70:48–60.
- McCarty MF, Lerner AJ. Nutraceuticals targeting generation and oxidant activity of peroxynitrite may aid prevention and control of Parkinson's disease. 2020;21:3624.
- Maiti P, Manna J, Dunbar GL (2017) Current understanding of the molecular mechanisms in Parkinson's disease: targets for potential treatments. *Transl Neurodegener* 6:28
- de Bie RMA, Clarke CE, Espay AJ, Fox SH, Lang AE (2020) Initiation of pharmacological therapy in Parkinson's disease: when, why, and how. *The Lancet Neurology* 19:452–461
- Fox SH, Katzenschlager R, Lim SY et al (2018) International Parkinson and movement disorder society evidence-based medicine review: update on treatments for the motor symptoms of Parkinson's disease. *Mov Disord* 33:1248–1266
- Forni C, Facchiano F, Bartoli M et al (2019) Beneficial role of phytochemicals on oxidative stress and age-related diseases. *Biomed Res Int* 2019:8748253–8748253
- Abuthawabeh R, Abuirmeleh AN, Alzoubi KH (2020) The beneficial effect of vanillin on 6-hydroxydopamine rat model of Parkinson's disease. *Restor Neurol Neurosci* 38:369–373
- Arya SS, Rookes JE, Cahill DM, Lenka SK (2021) Vanillin: a review on the therapeutic prospects of a popular flavouring molecule. *Advances in Traditional Medicine* 21:1–17
- Dhanalakshmi C, Janakiraman U, Manivasagam T et al (2016) Vanillin attenuated behavioural impairments, neurochemical deficits, oxidative stress and apoptosis against rotenone induced rat model of Parkinson's disease. *Neurochem Res* 41:1899–1910
- Kumar SS, Priyadarsini KI, Sainis KB (2004) Inhibition of peroxynitrite-mediated reactions by Vanillin. *J Agric Food Chem* 52:139–145
- Dhanalakshmi C, Manivasagam T, Nataraj J, Justin Thenmozhi A, Essa MM (2015) Neurosupportive role of Vanillin, a natural phenolic compound, on rotenone induced neurotoxicity in SH-SY5Y neuroblastoma cells. Evidence-based complementary and alternative Med eCAM 2015:626028
- Korecka JA, van Kesteren RE, Blaas E, Spitzer SO, Kamstra JH, Smit AB, Swaab DF, Verhaagen J, Bossers K (2013) Phenotypic characterization of retinoic acid differentiated SH-SY5Y cells by transcriptional profiling. *PLoS ONE* 8(5). <https://doi.org/10.1371/journal.pone.0063862>

23. Kim C, Park S (2018) IGF-1 protects SH-SY5Y cells against MPP(+)-induced apoptosis via PI3K/PDK-1/Akt pathway. *Endocr Connect* 7:443–455
24. Srivastav S, Anand BG, Fatima M et al (2020) Piperine-coated gold nanoparticles alleviate paraquat-induced neurotoxicity in *Drosophila melanogaster*. *ACS Chem Neurosci* 11:3772–3785
25. Fatima M, Ahmad MH, Srivastav S, Rizvi MA, Mondal AC (2020) A selective D2 dopamine receptor agonist alleviates depression through up-regulation of tyrosine hydroxylase and increased neurogenesis in hippocampus of the prenatally stressed rats. *Neurochem Int* 136:104730
26. Jackson-Lewis V, Przedborski S (2007) Protocol for the MPTP mouse model of Parkinson's disease. *Nat Protoc* 2:141–151
27. Matsuura K, Kabuto H, Makino H, Ogawa N (1997) Pole test is a useful method for evaluating the mouse movement disorder caused by striatal dopamine depletion. *J Neurosci Methods* 73:45–48
28. Chonpathompikunlert P, Boonruamkaew P, Sukketsiri W, Hutamekalin P, Sroyraya M (2018) The antioxidant and neurochemical activity of Apium graveolens L and its ameliorative effect on MPTP-induced Parkinson-like symptoms in mice. *BMC Complementary and Alternative Med* 18:103
29. Paxinos G, Franklin KBJ (2008) The mouse brain in stereotaxic coordinates. Academic Press, Third
30. Bradford MM (1976) A rapid and sensitive method for the quantitation of microgram quantities of protein utilizing the principle of protein-dye binding. *Anal Biochem* 72:248–254
31. Hilal Ahmad M, Fatima M, Hossain MM (2018) Mondal ACJ-JoB, Toxicology M Determination of potential oxidative damage, hepatotoxicity, and cytogenotoxicity in male Wistar rats. Role of Indomethacin 32:e22226
32. Ahmad MH, Fatima M, Ali M, Rizvi MA, Mondal AC (2021) Naringenin alleviates paraquat-induced dopaminergic neuronal loss in SH-SY5Y cells and a rat model of Parkinson's disease. *Neuropharmacology*. <https://doi.org/10.1016/j.neuropharm.2021.108831>
33. Kumar S, Srivastav S, Fatima M, Giri RS, Mandal B (2019) Mondal ACJJoAsD A synthetic pro-drug peptide reverses amyloid- $\beta$ -induced toxicity in the rat model of. *Alzheimer's Dis* 69:499–512
34. Gundersen HJ, Bendtsen TF, Korbo L, et al. Some new, simple and efficient stereological methods and their use in pathological research and diagnosis. *APMIS: acta pathologica, microbiologica, et immunologica Scandinavica* 1988;96:379–394.
35. Mironov A (2017) Stereological morphometric grids for ImageJ. *Ultrastruct Pathol* 41:126
36. Schindelin J, Arganda-Carreras I, Frise E et al (2012) Fiji: an open-source platform for biological-image analysis. *Nat Methods* 9:676–682
37. Langston JW (2017) The MPTP Story. *J Parkinson's Dis* 7:S11–S19
38. Aryal S, Skinner, T. Bridges, B. Weber, J. T. The pathology of Parkinson's disease and potential benefit of dietary polyphenols. *Molecules (Basel, Switzerland)* 2020;25.
39. Yan X, Liu DF, Zhang XY, et al. Vanillin protects dopaminergic neurons against inflammation-mediated cell death by inhibiting ERK1/2, P38 and the NF- $\kappa$ B signaling pathway. *Int J Mol Sci* 2017;18.
40. Kovalevich J, Langford D (2013) Considerations for the use of SH-SY5Y neuroblastoma cells in neurobiology. Springer, *Neuronal Cell Culture*, pp 9–21
41. More SV, Choi D-KJjoms. Atractylenolide-i protects human sh-sy5y cells from 1-methyl-4-phenylpyridinium-induced apoptotic cell death. 2017;18:1012.
42. Bezerra-Filho CSM, Barboza JN, Souza MTS, Sabry P, Ismail NSM, de Sousa DP (2019) Therapeutic potential of Vanillin and its main metabolites to regulate the inflammatory response and oxidative stress. *Mini Rev Med Chem* 19:1681–1693
43. Chanthammachat P, Dharmasaroja PJEj. Metformin restores the mitochondrial membrane potentials in association with a reduction in TIMM23 and NDUFS3 in MPP+-induced neurotoxicity in SH-SY5Y cells. 2019;18:812.
44. Yıldızhan K, Nazıroğlu M (2022) Protective role of selenium on MPP(+) and homocysteine-induced TRPM2 channel activation in SH-SY5Y cells. *J Recept Signal Transduct Res* 42:399–408
45. Naz H, Tarique M, Khan P et al (2018) Evidence of vanillin binding to CAMKIV explains the anti-cancer mechanism in human hepatic carcinoma and neuroblastoma cells. *Mol Cell Biochem* 438:35–45
46. Sefi M, Elwej A, Chaabane M et al (2019) Beneficial role of vanillin, a polyphenolic flavoring agent, on maneb-induced oxidative stress. DNA damage, and liver histological changes in Swiss albino mice 38:619–631
47. Salau VFEO, Ibeji CU, Olasehinde TA, Koorbanally NA, Islam MS (2020) Vanillin and vanillic acid modulate antioxidant defense system via amelioration of metabolic complications linked to Fe(2+)-induced brain tissues damage. *Metab Brain Dis* 35:727–738
48. Oladimeji OH, Njinga S, Abdullahi ST. Evaluation of antioxidant activity of obtained derivatives of vanillin. *Journal of Pharmaceutical Research Science & Technology [ISSN: 2583–3332]* 2022;6:17–25.
49. Huang D, Xu J, Wang J, et al. dynamic changes in the nigrostriatal pathway in the MPTP mouse model of Parkinson's disease. *Parkinson's Disease* 2017;2017:9349487.
50. Torres ERS, Akinyeke T, Stagaman K et al (2018) Effects of sub-chronic MPTP exposure on behavioral and cognitive performance and the microbiome of wild-type and mGlu8 knockout female and male mice. *Front Behav Neurosci* 12:140
51. Abdulrahman AA, Faisal K, Meshref AAA, Arshaduddin M (2017) Low-dose acute vanillin is beneficial against harmaline-induced tremors in rats. *Neurol Res* 39:264–270
52. Rani L, Mondal AC (2020) Emerging concepts of mitochondrial dysfunction in Parkinson's disease progression: pathogenic and therapeutic implications. *Mitochondrion* 50:25–34
53. Jiang P, Scarpa JR, Gao VD, Vitaterna MH, Kasarskis A, Turek FW (2019) Parkinson's disease is associated with dysregulations of a dopamine-modulated gene network relevant to sleep and affective neurobehaviors in the striatum. *Sci Rep* 9:4808
54. Duda P, Wiśniewski J, Wójtowicz T et al (2018) Targeting GSK3 signaling as a potential therapy of neurodegenerative diseases and aging. *Expert Opin Ther Targets* 22:833–848
55. Yang K, Chen Z, Gao J et al (2017) The key roles of GSK-3 $\beta$  in regulating mitochondrial activity. *Cell Physiol Biochem* 44:1445–1459
56. Li J, Ma S, Chen J et al (2020) GSK-3 $\beta$  contributes to parkinsonian dopaminergic neuron death: evidence from conditional knockout mice and tideglusib. *Front Mol Neurosci* 13:81
57. Zhang J, Liu W, Wang Y, Zhao S, Chang NJDm. miR-135b plays a neuroprotective role by targeting GSK3 $\beta$  in MPP+-intoxicated SH-SY5Y Cells. 2017;2017.
58. Ma W, Li X, Song P, et al. A vanillin derivative suppresses the growth of HT29 cells through the Wnt/ $\beta$ -catenin signaling pathway. 2019;849:43–49.
59. Pascal JM (2018) The comings and goings of PARP-1 in response to DNA damage. *DNA Repair* 71:177–182
60. Martire S, Mosca L, d'Erme MJMoa, development. PARP-1 involvement in neurodegeneration: a focus on Alzheimer's and Parkinson's diseases. 2015;146:53–64.
61. Mao K, Chen J, Yu H et al (2020) Poly (ADP-ribose) polymerase 1 inhibition prevents neurodegeneration and promotes  $\alpha$ -synuclein

- degradation via transcription factor EB-dependent autophagy in mutant  $\alpha$ -synucleinA53T model of Parkinson's disease. *Aging Cell* 19:e13163
62. Espinoza-Derout J, Shao XM, Bankole E et al (2019) Hepatic DNA Damage induced by electronic cigarette exposure is associated with the modulation of NAD<sup>+</sup>/PARP1/SIRT1 Axis. *Front Endocrinol* 10:320
  63. Enogieru AB, Haylett W, Hiss DC, Ekpo OEJMBD. Regulation of AKT/AMPK signaling, autophagy and mitigation of apoptosis in Rutin-pretreated SH-SY5Y cells exposed to MPP<sup>+</sup>. 2021;36:315–326.
  64. Sirangelo IS, L. Ragone, A. Naviglio, S. Iannuzzi, C. Vanillin prevents doxorubicin-induced apoptosis and oxidative stress in rat H9c2 cardiomyocytes. 2020;12.
  65. Lee Y-S, Kalimuthu K, Park YS, et al. BAX-dependent mitochondrial pathway mediates the crosstalk between ferroptosis and apoptosis. 2020;25:625–631.
  66. Blandino G, Valenti F, Sacconi A, Di Agostino S. Wild type- and mutant p53 proteins in mitochondrial dysfunction: emerging insights in cancer disease. 2020 2020: Elsevier: 105–117.
  67. Nkpaa KW, Awogbindin IO, Amadi BA, et al. Ethanol exacerbates manganese-induced neurobehavioral deficits, striatal oxidative stress, and apoptosis via regulation of p53, caspase-3, and bax/bcl-2 ratio-dependent pathway. 2019;191:135–148.
  68. Liu H, Wang J, Zhang Q, Geng L, Yang Y, Wu N (2020) Protective effect of fucoidan against MPP<sup>+</sup>-induced SH-SY5Y cells apoptosis by affecting the PI3K/Akt pathway. *Mar Drugs* 18:333
  69. Kawahata I, Fukunaga K. Degradation of tyrosine hydroxylase by the ubiquitin-proteasome system in the pathogenesis of Parkinson's disease and dopa-responsive dystonia. *Int J Mol Sci* 2020;21.
  70. Cobb CA, Cole MP (2015) Oxidative and nitrate stress in neurodegeneration. *Neurobiol Dis* 84:4–21
  71. Chidambaram SB, Bhat A, Ray B, et al. Cocoa beans improve mitochondrial biogenesis via PPAR $\gamma$ /PGC1 $\alpha$  dependent signaling pathway in MPP<sup>+</sup> intoxicated human neuroblastoma cells (SH-SY5Y). 2020;23:471–480.
  72. Roostalu U, Salinas CB, Thorbek DD, et al. Quantitative whole-brain 3D imaging of tyrosine hydroxylase-labeled neuron architecture in the mouse MPTP model of Parkinson's disease. *Disease models & mechanisms* 2019;12:dmm042200.
  73. Alam G, Edler M, Burchfield S, Richardson JR (2017) Single low doses of MPTP decrease tyrosine hydroxylase expression in the absence of overt neuron loss. *Neurotoxicology* 60:99–106
  74. Peng S, Wang C, Ma J et al (2018) *Achyranthes bidentata* polypeptide protects dopaminergic neurons from apoptosis in Parkinson's disease models both in vitro and in vivo. *Br J Pharmacol* 175:631–643

**Publisher's Note** Springer Nature remains neutral with regard to jurisdictional claims in published maps and institutional affiliations.

Springer Nature or its licensor (e.g. a society or other partner) holds exclusive rights to this article under a publishing agreement with the author(s) or other rightsholder(s); author self-archiving of the accepted manuscript version of this article is solely governed by the terms of such publishing agreement and applicable law.